

國立臺灣大學理學院物理學系

碩士論文

Department of Physics

College of Science

National Taiwan University

Master Thesis



即時熱輔助佔據密度泛函理論

Real-Time Thermally Assisted-Occupation Density
Functional Theory

蔡弘毅

Hung-Yi Tsai

指導教授: 蔡政達 博士

Advisor: Jeng-Da Chai, Ph.D.

中華民國 112 年 7 月

July, 2023





摘要

密度泛函理論，特別是 Kohn–Sham(KS) 密度泛函理論，[1] 因其高計算效率成為量子計算領域被廣泛應用的方法。然而，KS 密度泛函理論假設了基態密度具有非交互作用純態勢可代表性，這甚至限制了精確的 KS 密度泛函理論處理多參考系統的能力。為了從根本擺脫此限制，熱輔助佔據密度泛函理論已被開發。[2–4] 模擬結果顯示，熱輔助佔據密度泛函理論在單參考系統表現類似 KS 密度泛函理論，在多參考系統則優於 KS 密度泛函理論。其中，熱輔助佔據密度泛函理論展現了藉由分數佔據軌域描述靜態關聯能的能力。

如同線性響應含時密度泛函理論和即時含時密度泛函理論，[5] 線性響應含時熱輔助佔據密度泛函理論已被提出並應用於獲取激發能。[6] 這篇論文將把熱輔助佔據密度泛函理論擴展為即時熱輔助佔據密度泛函理論，不做線性響應理論常見的微擾近似以求更廣的適用性。過去作品中未完好定義的 Hartree 交換關聯 theta 作用量泛函也會一併修正。我們應用模擬氫分子系統，並討論線性響應理論無法處理的高諧波產生。模擬結果顯示，適當 θ 的即時熱輔助佔據密度泛函理論在單參考系統表現類似即時含時密度泛函理論。在多參考系統，足夠大 θ 的即時熱輔助佔據密度泛函理論則修復了限制自旋表述與非限制自旋表述被破壞的對稱。

關鍵字：即時熱輔助佔據密度泛函理論、即時含時密度泛函理論、含時熱輔助佔據密度泛函理論





Abstract

Density functional theory (DFT), specifically Kohn–Sham DFT (KS-DFT),^[1] is a widespread method in the field of quantum computation due to its high computational efficiency. However, KS-DFT assumes the ground-state density to be non-interacting pure-state (NI-PS) v_s -representable, which limits the ability of even exact KS-DFT to handle multi-reference systems. To relieve this limitation, thermally assisted-occupation DFT (TAO-DFT) has been developed.^[2–4] Simulation results suggest that TAO-DFT performs similarly to KS-DFT for single-reference systems, while outperforming KS-DFT for multi-reference systems. In particular, TAO-DFT is shown to describe static correlation through fractional orbital occupations.

Similar to linear-response time-dependent DFT (LR-TD-DFT) and real-time time-dependent DFT (RT-TD-DFT),^[5] LR-TD-TAO-DFT has been proposed and utilized to extract excitation energies.^[6] In this thesis, we aim to extend TAO-DFT to real-time TAO-DFT. The often made small perturbation approximation in LR theory is dropped for uni-

versality. The ill-defined Hartree-exchange-correlation-theta (HXC θ) action functional in the previous work is also revised. Specifically, we apply RT-TAO-DFT to hydrogen molecules. The phenomenon of high harmonic generation (HHG), which falls outside the scope of LR theory, is simulated and discussed. Simulation results suggest that RT-TAO-DFT with suitable θ performs similar to RT-TD-DFT for single-reference systems. While for multi-reference systems, RT-TAO-DFT with sufficiently large θ fixes the symmetry-breaking issue between spin-restricted and spin-unrestricted formulations.

Keywords: real-time thermally assisted-occupation density functional theory, real-time time-dependent density functional theory, time-dependent thermally assisted-occupation density functional theory



Contents

| | Page |
|--|------------|
| 摘要 | i |
| Abstract | iii |
| Contents | v |
| List of Figures | vii |
| Chapter 1 Introduction | 1 |
| Chapter 2 Theory | 11 |
| 2.1 Ground-State TAO-DFT | 11 |
| 2.2 LR-TD-TAO-DFT | 14 |
| 2.3 From Generalizations of Theorems to RT-TAO | 16 |
| 2.4 Expression of the TAO Ensemble | 19 |
| 2.5 From One-Electron States to a Basis of Fock Space | 21 |
| 2.6 Ensemble Average Evaluated by One-Electron States | 26 |
| 2.7 Expression of the RT-TAO Potential | 31 |
| 2.8 Some Details of Derivations | 35 |
| 2.9 Approximations for the HXC θ Potential | 37 |
| 2.10 Practical Scheme of RT-TAO | 38 |



| | | |
|---|--|----|
| Chapter 3 | Results | |
| 3.1 | High Harmonic Generation | 43 |
| 3.2 | Time-Dependent Observables | 43 |
| 3.3 | Computational Details | 45 |
| 3.4 | H_2 at the Equilibrium Geometry | 48 |
| 3.5 | H_2 at the Stretched Geometry | 52 |
| 3.6 | Discussions of Symmetry-Breaking Effects | 53 |
| Chapter 4 | Conclusions | 57 |
| References | | 61 |
| Appendix A — Systems Perpendicular to the Laser Polarization | | 67 |
| Appendix B — HHG Spectra without Window Functions | | 75 |



List of Figures

| | | |
|-------------|---|----|
| Figure 3.1 | Electric field of the impulse | 47 |
| Figure 3.2 | HHG spectra of H_2 at 1.45 a.u. | 49 |
| Figure 3.3 | Induced dipole moment of H_2 at 1.45 a.u. | 50 |
| Figure 3.4 | Number of bound electrons of H_2 at 1.45 a.u. | 51 |
| Figure 3.5 | HHG spectra of H_2 at 3.78 a.u. | 52 |
| Figure 3.6 | Induced dipole moment of H_2 at 3.78 a.u. | 54 |
| Figure 3.7 | Number of bound electrons of H_2 at 3.78 a.u. | 55 |
| Figure A.1 | HHG spectra of H_2 at 1.45 a.u. aligned perpendicular | 68 |
| Figure A.2 | Induced dipole moment of H_2 at 1.45 a.u. aligned perpendicular | 69 |
| Figure A.3 | Number of bound electrons of H_2 at 1.45 a.u. aligned perpendicular | 70 |
| Figure A.4 | HHG spectra of H_2 at 3.78 a.u. aligned perpendicular | 71 |
| Figure A.5 | Induced dipole moment of H_2 at 3.78 a.u. aligned perpendicular | 72 |
| Figure A.6 | Number of bound electrons of H_2 at 3.78 a.u. aligned perpendicular | 73 |
| Figure B.7 | HHG spectra of H_2 at 1.45 a.u. without window function | 76 |
| Figure B.8 | HHG spectra of H_2 at 3.78 a.u. without window function | 77 |
| Figure B.9 | HHG spectra of H_2 at 1.45 a.u. aligned perpendicular without window function | 78 |
| Figure B.10 | HHG spectra of H_2 at 3.78 a.u. aligned perpendicular without window function | 79 |



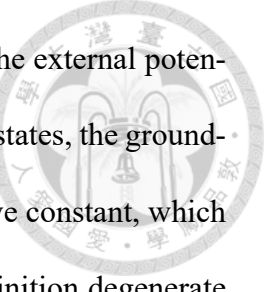


Chapter 1 Introduction

By applying the Born–Oppenheimer (BO) approximation,[7, 8] the positions of the atomic nuclei are considered as predetermined fixed parameters. Ideally, the famous Schrödinger equation can be solved for the ground state(s) and excited states to extract relevant information of physical interest. However, even with the BO approximations, the Schrödinger equation is only exactly solvable for a few of simple systems. For most systems, applying numerical methods is a must and only approximated solutions are obtained.

Configuration interaction (CI) and coupled cluster (CC) are popular wave function-based methods which provide rather accurate approximated solutions. They are known for systematically improvability and exactness at the limit of complete bases. However, the computational cost grows rapidly as system enlarges, limiting applicable systems to small or medium ones. Differently, density functional theory (DFT) transforms the wave function problems to ground-state electron density ones, which are less computationally demanding. In comparison, while wave function-based methods are often considered to be more accurate than DFT, the superior efficiency and reasonable accuracy of DFT make it possibly the only viable methods for large systems.

The theoretical basis of DFT relies on the Hohenberg–Kohn (HK) theorems,[9] which



establish a one-to-one mapping between the ground-state density and the external potential up to an additive constant. Moreover, even with degenerate ground states, the ground-state densities each maps to the same external potential up to an additive constant, which in turn uniquely determines the Hamiltonian.[10] Now because by definition degenerate states share the same energies, the possible one-to-many mapping between the Hamiltonian and the possible degenerate states leads to nothing but a one-to-one mapping between the Hamiltonian and the ground-state or excitation energies. Ground-state and excitation energies still can be written as functionals of the ground-state density. Therefore, if only the ground-state or excitation energies or any other density-related observable of the particular ground state is of interest, the problem becomes finding the particular ground-state density and the energy functionals of the ground-state density, hence the name of the theory.

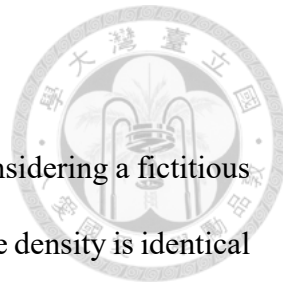
To find the ground-state density, the HK theorems provide a variational principle. The ground-state energy functional of a system consists of a system-dependent external potential term and a system-independent universal functional. The ground-state energy functional gives the global minimum if and only if the input density is (one of) the ground-state density(ies) associated with the external potential. In other words, after inserting all reasonable densities (any non-negative differentiable function that gives the correct electron number[11] under the constrained search formulation[12, 13]), the one(s) that give(s) the minimum is(are) the ground-state density(ies) associated with the external potential. DFT is a formally exact theory, with the inexactness arising from the unknown and thus necessarily approximated universal functional. The universal functional contains all system-indepedednt energy contributions, which equals to the sum of the interacting kinetic energy and the electron-electron repulsion energy. Of which, the approximations

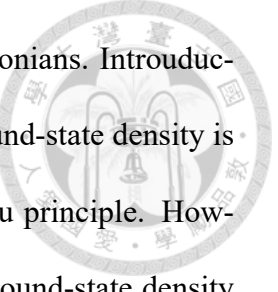
for the kinetic energy often lead to significant errors.[8, 14]

Kohn–Sham DFT (KS-DFT)[1] circumvents this problem by considering a fictitious non-interacting system, whose (assumed non-degenerate) ground-state density is identical to the (assumed non-degenerate) true ground-state density in the true interacting system. This consideration is equivalent to assuming that the true ground-state density can be represented by a pure (assumed non-degenerate) ground state of a non-interacting Hamiltonian with potential v_s (i.e., non-interacting pure-state (NI-PS) v_s -representable). If this assumption holds, by the HK theorems, the corresponding external potential of the non-interacting system is uniquely determined up to an additive constant, known as the KS potential. The form of the KS potential (which depends on the ground-state density) is provided in KS-DFT. However, since the ground-state density is unknown prior to simulations, a self-consistent scheme with a reasonable guessed density is often required.

KS-DFT is a formally exact theory, with the inexactness arising from the unknown and thus necessarily approximated exchange–correlation (XC) energy functional. The advantage of KS-DFT is that the (non-interacting) kinetic energy is treated exactly with the introduction of KS orbitals (see below), which are preferred over the unknown and thus necessarily approximated density functional of non-interacting kinetic energy.[8] To sum up, the problem of finding the true ground-state density in the true interacting system and the ground-state energy functional, is transformed into finding the ground-state density in the fictitious non-interacting system and the XC functional, which is easier for the non-interacting nature and more accurate for the exact treatment of the non-interacting kinetic energy.

In KS-DFT, owing to the non-interacting nature of the fictitious system, the multi-



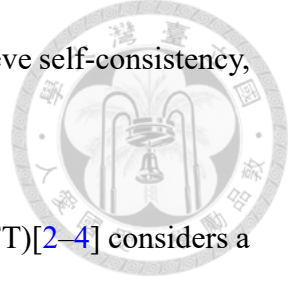


electron Hamiltonian can be written as the sum of one-electron Hamiltonians. Introducing so-called KS orbitals as a basis, for a N_{el} -electron system, the ground-state density is obtained by filling the lowest N_{el} KS orbitals according to the Aufbau principle. However, not all densities are NI-PS v_s -representable.[13, 15–18] If the ground-state density is not NI-PS v_s -representable, then even the exact KS-DFT would fail to achieve self-consistency, otherwise the density is by definition NI-PS v_s -representable and contradicts the premise.

Given a complete set of atomic or molecular orbitals, the exact N_{el} -electron wave function can be exactly expanded as a linear combination of many Slater determinants, each constructed with N_{el} of the orbitals. If the wave function is predominantly one determinant, it is termed a “single-reference” wave function. Otherwise, if the wave function has primary contributions of multiple determinants, it is termed a “multi-reference” wave function. For our interest, the exact ground-state wave function is primarily dominated by the determinant with the lowest energy. In this case, if low-energy determinants or high-energy determinants non-negligibly contribute, it is said to have strong “static correlation” or “dynamic correlation”, respectively.[19] Such systems are sometimes called “strongly correlated systems.” While the descriptions of “low energy” and “high energy” are somewhat ambiguous that the static correlation and the dynamic correlation are not clearly separable, in many cases the static correlation is associated with degenerate or nearly degenerate determinants. Such determinants are not preferred over the others, and the corresponding distributions of electrons are static in the sense that we term it ”static correlation.”

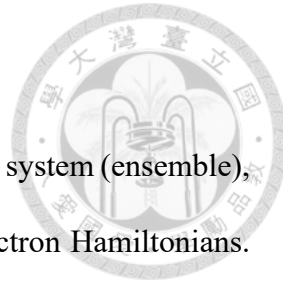
While we are not to conclude none of the ground-state densities of multi-reference systems is NI-PS v_s -representable, it is often true that such densities are not NI-PS v_s -

representable.[16] In such cases, even the exact KS-DFT fails to achieve self-consistency, as mentioned above.



On the other hand, thermally assisted-occupation DFT (TAO-DFT)[2–4] considers a fictitious non-interacting system (ensemble) at temperature θ whose ground-state density is identical to the (assumed non-degenerate) true ground-state density in the true interacting system. TAO-DFT assumes the true ground-state density to be non-interacting thermal ensemble (NI-TE) v_s -representable, rather than NI-PS v_s -representable as assumed in KS-DFT. The assumption of NI-TE v_s -representability is more likely to hold because NI-PS v_s -representability implies NI-TE v_s -representability, but not vice versa. If the assumption of NI-TE v_s -representability holds, by Mermin’s theorems,[20] the corresponding external potential of the non-interacting system (ensemble) is uniquely determined up to an additive constant, known as the TAO potential. The form of the TAO potential (which depends on the ground-state density) is provided in TAO-DFT. However, since the ground-state density is unknown prior to simulations, a self-consistent scheme with a reasonable guessed density is often required.

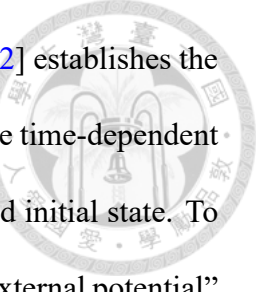
TAO-DFT is a formally exact theory, with the inexactness arising from the unknown and thus necessarily approximated XC energy functional and the θ -dependent energy functional. The advantage of TAO-DFT is that it performs similarly to KS-DFT for single-reference systems, while outperforming KS-DFT for multi-reference systems, with a cost comparable to KS-DFT.[2] To sum up, the problem of finding the true ground-state density in the true interacting system and the ground-state energy functional, is transformed into finding the ground-state density in the fictitious non-interacting system (ensemble) at temperature θ , the XC functional, and the θ functional, which is easier for the same reason as KS-DFT. It is worth mentioning that when θ is set to zero, TAO-DFT reduces to



In TAO-DFT, owing to the non-interacting nature of the fictitious system (ensemble), the multi-electron Hamiltonian can be written as the sum of one-electron Hamiltonians. Introducing so-called TAO orbitals as a basis, for a N_{el} -electron system, the ground-state density is obtained by filling TAO orbitals according to the Fermi–Dirac distribution.[\[21–23\]](#) For multi-reference systems, where even the exact KS-DFT may fail, TAO-DFT has been shown to describe static correlation through fractional orbital occupations.

Various XC functionals and θ functionals have been adopted in TAO-DFT, including the local density approximation (LDA),[\[2\]](#) the generalized-gradient approximation (GGA),[\[3\]](#) and hybrid functionals.[\[4, 24\]](#) Self-consistent schemes to determine system-dependent θ [\[25\]](#) and a simple model to determine system-independent θ [\[26\]](#) have been proposed. *Ab initio* molecular dynamics (AIMD) combined with TAO-DFT have been used to study dynamical properties.[\[27\]](#) For practical applications, numerous systems have been studied.[\[28–41\]](#)

To summarize, the goal is to solve the time-independent Schrödinger equation, which leads to the development of KS-DFT and TAO-DFT for their balance performance between cost and accuracy. However, KS-DFT and TAO-DFT are limited to the ground-state energy or any other density-related observables of the ground state, despite theoretically being able to determine excitation energies.[\[10\]](#) Naturally, if the goal is to solve the time-dependent Schrödinger equation for the time-dependent state with a given initial state, we expect an extension of DFT. Hence comes time-dependent (TD) DFT, which not only allows for the general study of time-dependent dynamics, but also enables determinations of excitation energies.



As the HK theorems are to DFT, the Runge–Gross (RG) theorem[42] establishes the one-to-one mapping between the time-dependent electron density and the time-dependent external potential up to a time-dependent additive function, for any fixed initial state. To clarify, “the time-dependent electron density” and “the time-dependent external potential” refer to the electron density and the external potential at all times between the initial time t_0 and the final time t_1 , not just at some instants between. In other words, given any fixed initial state, the time-dependent density uniquely determines the time-dependent external potential up to a time-dependent additive function, along with the time-dependent Hamiltonian, the time-dependent wave function, and all time-dependent observables. Therefore, while it may be hard to explicitly write down the mappings, the mappings do exist and all time-dependent observables can be written as functionals of the time-dependent density and the fixed initial state.[8] The original problem of solving for the time-dependent state is equivalent to find the time-dependent density and the relevant density functionals, similar to ground-state DFT.

To find the density functional is a comprehensive topic. The simplest one is the time-dependent density itself, then ones directly obtainable from the time-dependent density (e.g., the dipole moment and the number of electrons). The time-dependent density is the fundation of the whole theory, and we will focus on this part.

Impressed by the power of KS-DFT, we would like to develop a KS-like TD-DFT scheme. Specifically, given an initial state $|\Psi(t_0)\rangle$ to find the time-dependent density, we consider a fictitious non-interacting system with an initial state $|\Psi'(t_0)\rangle$ that produces the true time-dependent density in the true interacting system. Thus comes the van Leeuwen theorem,[43] which says if the chosen initial state $|\Psi'(t_0)\rangle$ produces the true initial density and the true initial time derivative of the density, then the external potential of the non-

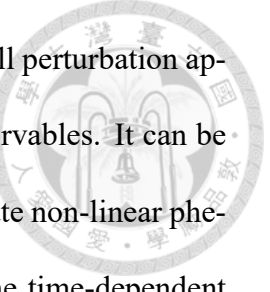
interacting system producing the true time-dependent density in the true interacting system exists and is uniquely determined up to an additive constant, known as the TDKS potential.

The form of the TDKS potential is provided by Runge and Gross.[42]

TD-DFT is a formally exact theory, with the inexactness arising from the unknown and thus necessarily approximated XC action functional. To sum up, given an initial state $|\Psi(t_0)\rangle$, the problem of finding the true time-dependent density in the true interacting system, is transformed into finding the XC action functional and an initial state $|\Psi'(t_0)\rangle$ satisfying the aforementioned conditions, propagating the initial state $|\Psi'(t_0)\rangle$ to get the time-dependent state $|\Psi'(t)\rangle$, and evaluating the time-dependent density in the fictitious non-interacting system.

While not strictly necessary, in most applications the given (assigned) initial state $|\Psi(t_0)\rangle$ is the (assumed non-degenerate) ground state. Because in such cases, we may use KS-DFT to find the initial state $|\Psi'(t_0)\rangle$ that produces the true ground-state density and zero time derivative of the density. However, as mentioned previously, even the exact KS-DFT may fail in multi-reference systems. This underscores the importance of alternative methods as TAO-DFT and its TD-extension, which handle such challenging systems in a more reliable framework.

TD-DFT is a powerful method for simulating systems with time-dependent external potentials, belonging to which linear-response (LR) TD-DFT is widely used to extract low-lying excitation energies. In LR-TD-DFT, one assumes that the external potential is weakly perturbed (small perturbation approximation). By studying the response of the system, i.e., solving the linear-response equations, excitation energies and transition densities are extracted.



On the other hand, real-time (RT) TD-DFT does not make the small perturbation approximation and in principle allow for finding all time-dependent observables. It can be used to find excitation energies (including high-lying ones) or to simulate non-linear phenomena, e.g., high harmonic generation (HHG).^[5] In RT-TD-DFT, the time-dependent density is explicitly obtained, which enables the studying of electron dynamics, photochemistry, laser–matter interaction, and so on.

As the similarities between TAO-DFT and KS-DFT, the TAO version of LR-TD-DFT, namely LR-TD-TAO-DFT or simply TDTAO, has been proposed and used to extract low-lying excitation energies.^[6] However, because of the missing definition of the TAO wave function in the previous work, the Hartree–exchange–correlation–theta (HXC θ) action functional is ill-defined.

In this work, we aim to address the issue of the ill-defined HXC θ action functional, and to propose the TAO version of RT-TD-DFT, namely RT-TD-TAO-DFT. We will refer to this new theory as RT-TAO to distinguish it from TDTAO. To assess RT-TAO, HHG is simulated for hydrogen molecules, and we would compare the results with those from RT-TD-DFT. We will refer to KS-DFT, LR-TD-DFT, and RT-TD-DFT as KS schemes, and refer to TAO-DFT, TDTAO, and RT-TAO as TAO schemes.





Chapter 2 Theory

2.1 Ground-State TAO-DFT

Here we give a review of ground-state TAO-DFT, adapting from the work of Chai.[2–4] This serves as a refresher for those familiar with ground-state TAO-DFT.

TAO-DFT aims to determine the (assumed non-degenerate) true ground-state density of an interacting system by finding the ground-state density in a fictitious non-interacting system (ensemble). In the spin-restricted formulation, the procedure is as follows:

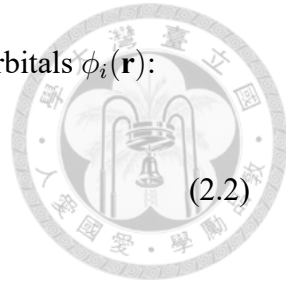
1. Choose a value for θ . System-independent values provided by a simple model may be a good option.[26]
2. Initialize the density $n_0(\mathbf{r})$ with a guessed density.
3. Construct the TAO potential $v_s(\mathbf{r})$ using the expression:

$$v_s(\mathbf{r}) = v(\mathbf{r}) + \int d^3r' \frac{n_0(\mathbf{r}')}{\|\mathbf{r} - \mathbf{r}'\|} + \frac{\delta E_{XC}^{\text{KS}}[n_0]}{\delta n_0(\mathbf{r})} + \frac{\delta E_\theta[n_0]}{\delta n_0(\mathbf{r})} \quad (2.1)$$

where $v(\mathbf{r})$ is the external potential, $E_{XC}^{\text{KS}}[n_0]$ is the exchange–correlation functional defined in KS-DFT, and $E_\theta[n_0]$ is defined in TAO-DFT.

4. Solve the following equation for orbital energies ϵ_i and TAO orbitals $\phi_i(\mathbf{r})$:

$$\left(-\frac{1}{2} \nabla_{\mathbf{r}}^2 + v_s(\mathbf{r}) \right) \phi_i(\mathbf{r}) = \epsilon_i \phi_i(\mathbf{r}) \quad (2.2)$$



5. For a N_{el} -electron system, solve the equation:

$$\sum_{i=1}^{\infty} \{1 + \exp[(\epsilon_i - \mu)/\theta]\}^{-1} = N_{\text{el}} \quad (2.3)$$

for the chemical potential μ .

6. Determine the occupation numbers f_i using:

$$f_i = \{1 + \exp[(\epsilon_i - \mu)/\theta]\}^{-1} \quad (2.4)$$

7. Update the density $n_0(\mathbf{r})$ according to:

$$n_0(\mathbf{r}) = \sum_{i=1}^{\infty} f_i \phi_i^*(\mathbf{r}) \phi_i(\mathbf{r}) \quad (2.5)$$

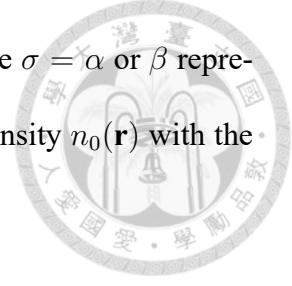
8. Repeat steps 3 to 7 until achieving self-consistency (i.e., the difference between the old and the new $n_0(\mathbf{r})$ is negligible).

9. The most recent $n_0(\mathbf{r})$ is the true ground-state density in the true interacting system.

For the spin-unrestricted formulation, the procedure is similar to the spin-restricted one with a few modifications:

1. Choose a value for θ . System-independent values provided by a simple model may be a good option.[26]

2. Initialize the spin densities $n_0^\sigma(\mathbf{r})$ with guessed densities, where $\sigma = \alpha$ or β represents spin-up or spin-down, respectively. Initialize the total density $n_0(\mathbf{r})$ with the sum of the spin densities:



$$n_0(\mathbf{r}) = n_0^\alpha(\mathbf{r}) + n_0^\beta(\mathbf{r}) \quad (2.6)$$

3. Construct the TAO potentials $v_s^\sigma(\mathbf{r})$ using the expressions:

$$v_s^\sigma(\mathbf{r}) = v(\mathbf{r}) + \int d^3r' \frac{n_0(\mathbf{r}')}{\|\mathbf{r} - \mathbf{r}'\|} + \frac{\delta E_{\text{XC}}^{\text{KS}}[n_0^\alpha, n_0^\beta]}{\delta n_0^\sigma(\mathbf{r})} + \frac{\delta E_\theta[n_0^\alpha, n_0^\beta]}{\delta n_0^\sigma(\mathbf{r})} \quad (2.7)$$

where $v(\mathbf{r})$ is the external potential, $E_{\text{XC}}^{\text{KS}}[n_0^\alpha, n_0^\beta]$ is the exchange–correlation functional defined in KS-DFT, and $E_\theta[n_0^\alpha, n_0^\beta]$ is defined in TAO-DFT.

4. Solve the following equations for orbital energies ϵ_i^σ and spin TAO orbitals $\phi_i^\sigma(\mathbf{r})$:

$$\left(-\frac{1}{2} \nabla_{\mathbf{r}}^2 + v_s^\sigma(\mathbf{r}) \right) \phi_i^\sigma(\mathbf{r}) = \epsilon_i^\sigma \phi_i^\sigma(\mathbf{r}) \quad (2.8)$$

5. For a system with N_{el}^α spin-up electrons and N_{el}^β spin-down electrons, solve the equations:

$$\sum_{i=1}^{\infty} \{1 + \exp[(\epsilon_i^\sigma - \mu_\sigma)/\theta]\}^{-1} = N_{\text{el}}^\sigma \quad (2.9)$$

for the chemical potentials μ_σ .

6. Determine the occupation numbers f_i^σ using:

$$f_i^\sigma = \{1 + \exp[(\epsilon_i^\sigma - \mu_\sigma)/\theta]\}^{-1} \quad (2.10)$$

7. Update the spin densities $n_0^\sigma(\mathbf{r})$ by:

$$n_0^\sigma(\mathbf{r}) = \sum_{i=1}^{\infty} f_i^\sigma \phi_i^{\sigma*}(\mathbf{r}) \phi_i^\sigma(\mathbf{r}) \quad (2.11)$$



and update the total density $n_0(\mathbf{r})$ using eq. (2.6).

8. Repeat steps 3 to 7 until achieving self-consistency (i.e., the difference between the old and the new $n_0(\mathbf{r})$ is negligible).

9. The most recent $n_0(\mathbf{r})$ is the true ground-state density in the true interacting system.

2.2 LR-TD-TAO-DFT

In this section, our focus is to address a defect in the previous work.[6] When it comes to TD-DFT, it is crucial to approximate the XC action functional. Similarly, in TDTAO, we have to approximate the HXC θ action functional. The particular functional, denoted as $A_{\text{HXC}\theta}[n]$, holds a central position in TDTAO and is defined by:

$$A_{\text{HXC}\theta}[n] \equiv B_{\text{TAO}}[n] - B[n] \quad (2.12)$$

where

$$B_{\text{TAO}}[n] = A_{\text{TAO}}[n] + \int_{t_0}^{t_1} dt \int d^3r v_s(\mathbf{r}, t) n(\mathbf{r}, t) \quad (2.13)$$

and

$$B[n] = A[n] + \int_{t_0}^{t_1} dt \int d^3r v(\mathbf{r}, t) n(\mathbf{r}, t) \quad (2.14)$$

are universal action functionals. Here, $A_{\text{TAO}}[n]$ and $A[n]$ represent the total action functionals of the TAO system and the true interacting system, respectively, given by:

$$A_{\text{TAO}}[n] = \int_{t_0}^{t_1} dt \langle \Psi_{\text{TAO}}[n](t) | \left(i \frac{\partial}{\partial t} - \hat{H}_s(t) \right) | \Psi_{\text{TAO}}[n](t) \rangle \quad (2.15)$$

and

$$A[n] = \int_{t_0}^{t_1} dt \langle \Psi[n](t) | \left(i \frac{\partial}{\partial t} - \hat{H}(t) \right) | \Psi[n](t) \rangle \quad (2.16)$$

respectively. Here, $\Psi_{\text{TAO}}[n](t)$ and $\Psi[n](t)$, $\hat{H}_s(t)$ and $\hat{H}(t)$ are the wave functions and the Hamiltonians of the TAO system and the true interacting system, respectively.

However, please note the wave function of the TAO system (ensemble) $\Psi_{\text{TAO}}[n](t)$ is currently undefined, which consequently raises issues with the definition of $A_{\text{HXC}\theta}[n]$. This issue will be addressed in the subsequent sections.

Suppose we have the necessary approximations for $A_{\text{HXC}\theta}[n]$, and that $\Psi_{\text{TAO}}[n](t)$ is well-defined. In such case, the expression for $v_s(\mathbf{r}, t)$ is given by:

$$v_s(\mathbf{r}, t) = v(\mathbf{r}, t) + \frac{\delta A_{\text{HXC}\theta}[n]}{\delta n(\mathbf{r}, t)} + i \left\langle \Psi[n](t_1) \left| \frac{\delta \Psi[n; t_1]}{\delta n(\mathbf{r}, t)} \right. \right\rangle - i \left\langle \Psi_{\text{TAO}}[n](t_1) \left| \frac{\delta \Psi_{\text{TAO}}[n; t_1]}{\delta n(\mathbf{r}, t)} \right. \right\rangle \quad (2.17)$$

If we define $v_{\text{HXC}\theta}[n](\mathbf{r}, t)$ as:

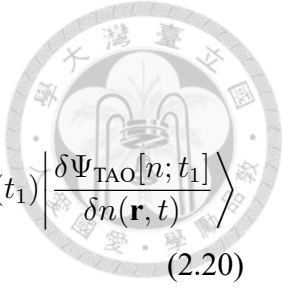
$$v_{\text{HXC}\theta}[n](\mathbf{r}, t) \equiv v_s(\mathbf{r}, t) - v(\mathbf{r}, t) \quad (2.18)$$

Using this definition, we can express $v_s(\mathbf{r}, t)$ as the sum of $v(\mathbf{r}, t)$ and $v_{\text{HXC}\theta}[n](\mathbf{r}, t)$:

$$v_s(\mathbf{r}, t) = v(\mathbf{r}, t) + v_{\text{HXC}\theta}[n](\mathbf{r}, t) \quad (2.19)$$

where $v_{\text{HXC}\theta}[n](\mathbf{r}, t)$ is given by:

$$v_{\text{HXC}\theta}[n](\mathbf{r}, t) = \frac{\delta A_{\text{HXC}\theta}[n]}{\delta n(\mathbf{r}, t)} + i \left\langle \Psi[n](t_1) \left| \frac{\delta \Psi[n; t_1]}{\delta n(\mathbf{r}, t)} \right. \right\rangle - i \left\langle \Psi_{\text{TAO}}[n](t_1) \left| \frac{\delta \Psi_{\text{TAO}}[n; t_1]}{\delta n(\mathbf{r}, t)} \right. \right\rangle \quad (2.20)$$



2.3 From Generalizations of Theorems to RT-TAO

The generalization of the HK theorems to grand canonical ensembles was accomplished by Mermin.[20] In such case, consider the temperature θ (which is the product of the Boltzmann constant k_B and the absolute temperature T_{el}) and the chemical potential μ , the equilibrium mixed state can be written as a functional of the equilibrium density. Li extended the RG theorems to ensembles.[44, 45] Given any fixed initial mixed state, the time-dependent mixed state can be written as a functional of the time-dependent density.

Furthermore, Pribram-Jones extended the van Leeuwen theorem to ensembles within LR region,[46] and Dufty extended it generally.[47] Although a complete characterization of the necessary conditions is not provided, these works demonstrate the existence and uniqueness of the external potential in the non-interacting system (ensemble) up to an additive constant that yields the true time-dependent density in the true interacting system.

For simplicity, we will neglect the consideration of electron spins in the following discussions, although it can be easily incorporated with appropriate treatment. Unless noted otherwise, atomic units are assumed.

As mentioned in chapter 1, our goal is to find the true time-dependent density in the true interacting system $n(\mathbf{r}, t)$. To achieve this, we aim to develop a RT-TAO scheme analogous to TD-DFT. Specifically, given an initial state $|\Psi(t_0)\rangle$, we consider a fictitious non-

interacting ensemble with an initial mixed state $\hat{\Gamma}_s(t_0)$ that yields the true time-dependent density $n(\mathbf{r}, t)$ in the true interacting system.

Similar to TD-DFT, while not strictly necessary, we will focus on the cases where the given (assigned) initial state $|\Psi(t_0)\rangle$ is the (assumed non-degenerate) ground state. Because in such cases, TAO-DFT can be used to find the initial mixed state $\hat{\Gamma}_s(t_0)$ that yields the true ground-state density $n(\mathbf{r}, t_0) = n_0(\mathbf{r})$ and zero time derivative of density $\frac{\partial n}{\partial t}(\mathbf{r}, t_0) = 0$. The initial mixed state $\hat{\Gamma}_s(t_0)$ is defined to be a grand canonical ensemble with the temperature θ and the chemical potential μ , which is implicit in TAO-DFT. The time-dependent TAO ensemble is then defined by propagating according to the time-dependent Schrödinger equation or the von Neumann equation. Because for $t > t_0$, the time-dependent mixed state $\hat{\Gamma}_s(t)$ in general deviates from equilibrium, we refer to this mixed state as the TAO ensemble to distinguish it from the equilibrium grand canonical ensemble.

Based on the generalization of the van Leeuwen theorem to ensembles,[47] we expect or assume the existence and uniqueness of the external potential $v_s(\mathbf{r}, t)$ in the non-interacting ensemble up to an additive constant that yields the true time-dependent density in the true interacting system. This potential is known as the RT-TAO potential. The form of the RT-TAO potential $v_s(\mathbf{r}, t)$ is provided in section 2.7.

RT-TAO is a formally exact theory, with the inexactness arising from the unknown and thus necessarily approximated $\text{XC}\theta$ action functional $A_{\text{XC}\theta}[n]$. Moreover, by the HK theorems,[9] the given (assigned) initial (assumed non-degenerate) ground state $|\Psi(t_0)\rangle$ can also be written as a functional of the ground state density $n_0(\mathbf{r}) = n(\mathbf{r}, t_0)$. In other words, the initial state $|\Psi(t_0)\rangle$ dependence can be incorporated into the time-dependent

density $n(\mathbf{r}, t)$. Apply this to the RG theorems,[42] we conclude all time-dependent properties can be written as functionals of the time-dependent density $n(\mathbf{r}, t)$ alone. Specifically, the time-dependent state $|\Psi(t)\rangle$ can be written as

$$|\Psi(t)\rangle = |\Psi[n](t)\rangle \quad (2.21)$$

To sum up, given (assigned) an initial state as the (assumed non-degenerate) ground state, the problem of finding the true time-dependent density $n(\mathbf{r}, t)$ in the true interacting system, is transformed into finding the XC θ functional $A_{XC\theta}[n]$ and an initial mixed state $\hat{\Gamma}_s(t_0)$ yielding the true initial density $n(\mathbf{r}, t_0) = n_0(\mathbf{r})$ and zero time derivative of the density $\frac{\partial n}{\partial t}(\mathbf{r}, t_0) = 0$ with TAO-DFT, propagating the initial mixed state $\hat{\Gamma}_s(t_0)$ to obtain the time-dependent mixed state $\hat{\Gamma}_s(t)$, and evaluating the time-dependent density $n(\mathbf{r}, t)$ in the fictitious non-interacting ensemble.

The form of the RT-TAO potential $v_s(\mathbf{r}, t)$ would be derived in section 2.7, with the problem of finding the XC θ functional $A_{XC\theta}[n]$ relieved if adopting the adiabatic approximation[8] (section 2.9). As for the other part, one may notice the explicit information of the initial mixed state $\hat{\Gamma}_s(t_0)$ or the time-dependent mixed state $\hat{\Gamma}_s(t)$ is unnecessary, but only the time-dependent density $n(\mathbf{r}, t)$ is of interest. In the following sections, we would move from the formulation of mixed states to one-electron states to benefit from its simplicity.



2.4 Expression of the TAO Ensemble

The Hamiltonian of the fictitious non-interacting ensemble can be written as[48, 49]

$$\hat{H}_s(t) = \bigoplus_{N=0}^{\infty} \hat{H}_s^N(t) \quad (2.22)$$

where the symbol “ \bigoplus ” denotes a direct sum, and

$$\hat{H}_s^N(t) = \hat{T}^N + \hat{V}_s^N(t) \quad (2.23)$$

is the N -electron Hamiltonian, with $\hat{H}_s^0(t) = 0$ (the vacuum state has no energy).[48, 49]

It includes the kinetic energy term

$$\hat{T}^N = \sum_{j=1}^N \left(-\frac{1}{2} \nabla_{\mathbf{r}_j}^2 \right) \quad (2.24)$$

and the RT-TAO potential term

$$\hat{V}_s^N(t) = \sum_{j=1}^N v_s(\mathbf{r}_j, t) \quad (2.25)$$

For instance, let $|u_s(t)\rangle$ denotes any element in this space:[48]

$$|u_s(t)\rangle = \bigoplus_{N=0}^{\infty} |u_s^N(t)\rangle \quad (2.26)$$

where $|u_s^N(t)\rangle$ is any element in the N -electron Hilbert space, with $|u_s^0(t)\rangle = |0\rangle$ the vacuum state.[48, 49] In such case, we have[48]

$$\hat{H}_s(t) |u_s(t)\rangle = \bigoplus_{N=0}^{\infty} \hat{H}_s^N(t) |u_s^N(t)\rangle \quad (2.27)$$

One may loosely understand as when acting on a N -electron state, the N -electron Hamiltonian should be used.[50]

To explicitly write down the time-dependent mixed state $\hat{\Gamma}_s(t)$, we introduce the states $|\Phi_k(t)\rangle$ that form a complete orthonormal basis, each with a definite energy E_k and a definite number of electrons N_k at the initial time:

$$\hat{H}_s(t_0) |\Phi_k(t_0)\rangle = E_k |\Phi_k(t_0)\rangle \quad (2.28)$$

Equation (2.28) implies that the initial states $|\Phi_k(t_0)\rangle$ are eigenstates of the initial Hamiltonian of the fictitious non-interacting ensemble $\hat{H}_s(t_0)$. An example of such a basis is provided in section 2.5.

Expressed in this basis, the initial density operator describing the initial mixed state $\hat{\Gamma}_s(t_0)$ (which is defined to be a grand canonical ensemble in section 2.3) is

$$\hat{\Gamma}_s(t_0) = \sum_{k=0}^{\infty} w_k |\Phi_k(t_0)\rangle\langle\Phi_k(t_0)| \quad (2.29)$$

where the weights w_k are time-independent and given by

$$w_k = \frac{e^{-(E_k - \mu N_k)/\theta}}{\sum_{l=0}^{\infty} e^{-(E_l - \mu N_l)/\theta}} \quad (2.30)$$

By the time-dependent Schrödinger equation

$$i\frac{\partial}{\partial t} |\Phi_k(t)\rangle = \hat{H}_s(t) |\Phi_k(t)\rangle \quad (2.31)$$

we can propagate the initial states $|\Phi_k(t_0)\rangle$ to get the time-dependent mixed state $\hat{\Gamma}_s(t)$:

$$\hat{\Gamma}_s(t) = \sum_{k=0}^{\infty} w_k |\Phi_k(t)\rangle\langle\Phi_k(t)| \quad (2.32)$$



This expression follows the definition of the time-dependent mixed state in the fictitious non-interacting ensemble given in section 2.3.

2.5 From One-Electron States to a Basis of Fock Space

Consider an one-electron Hamiltonian given by

$$\hat{h}_s(t) = -\frac{1}{2}\nabla_{\mathbf{r}}^2 + v_s(\mathbf{r}, t) \quad (2.33)$$

We can find a set of normalized one-electron states $|\phi_i(t)\rangle$, each initially having an orbital energy ϵ_i and containing one electron, such that they satisfy the time-independent Schrödinger equation:

$$\hat{h}_s(t_0) |\phi_i(t_0)\rangle = \epsilon_i |\phi_i(t_0)\rangle \quad (2.34)$$

By the time-dependent Schrödinger equation

$$i\frac{\partial}{\partial t} |\phi_i(t)\rangle = \hat{h}_s(t) |\phi_i(t)\rangle \quad (2.35)$$

we can propagate the initial one-electron states $|\phi_i(t_0)\rangle$ to get the time-dependent one-electron states $|\phi_i(t)\rangle$.

Since the initial one-electron states $|\phi_i(t_0)\rangle$ can be viewed as normalized eigenstates of the initial one-electron Hamiltonian $\hat{h}_s(t_0)$, they form a complete orthonormal basis for the one-electron Hilbert space.[51] It can be shown that the propagator $\hat{U}(t, t_0)$ which

transforms $|\phi_i(t_0)\rangle$ into $|\phi_i(t)\rangle$:

$$|\phi_i(t)\rangle = \hat{U}(t, t_0) |\phi_i(t_0)\rangle \quad (2.36)$$



remains unitary even with a time-dependent Hamiltonian $\hat{h}_s(t)$.^[51] Consequently, the time-dependent one-electron states $|\phi_i(t)\rangle$ preserve orthonormality and constantly form a complete orthonormal basis for the one-electron Hilbert space.

Next consider a normalized anti-symmetrized two-electron state. Because the system in consideration is non-interacting, we can directly fill up two orbitals, say $\phi_i(\mathbf{r}, t)$ and $\phi_j(\mathbf{r}, t)$. This state can be expressed as a Slater determinant:

$$|\phi_i\phi_j(t)\rangle_- = \frac{1}{\sqrt{2!}} (|\phi_i^1(t)\rangle \otimes |\phi_j^2(t)\rangle - |\phi_j^1(t)\rangle \otimes |\phi_i^2(t)\rangle) \quad (2.37)$$

Here, the symbol “ \otimes ” represents the direct product, and a general discussion including interaction can be found in the note of Solovej.^[48] The superscripts 1 and 2 are appended to emphasize the respective electron. We now claim the states $|\Phi_0(t)\rangle = |0\rangle$, $|\Phi_1(t)\rangle = |\phi_1(t)\rangle$, $|\Phi_2(t)\rangle = |\phi_2(t)\rangle$, \dots , $|\Phi_3(t)\rangle = |\phi_1\phi_2(t)\rangle_-$, $|\Phi_4(t)\rangle = |\phi_1\phi_3(t)\rangle_-$, \dots form a basis satisfying all the conditions specified in section 2.4.

Since the one-electron states $|\phi_i(t)\rangle$ form a complete orthonormal basis for the one-electron Hilbert space, the two-electron states $|\phi_i\phi_j(t)\rangle_-$ form a complete orthonormal basis for the two-electron Hilbert space. Similarly, the three-electron states $|\phi_i\phi_j\phi_l(t)\rangle_-$ form a complete orthonormal basis for the three-electron Hilbert space, and so on. Therefore, the states $|\Phi_k(t)\rangle$ defined above, including the vacuum state, one-electron states, and anti-symmetrized multi-electron states, form a complete basis for the Fock space.

As for the orthonormality, knowing the states $|\Phi_k(t)\rangle$ can be expressed as a linear

combination of the basis:

$$|\Phi_k(t)\rangle = a^k |0\rangle \oplus \sum_{i=0}^{\infty} a_i^k |\phi_i(t)\rangle \oplus \sum_{i=0}^{\infty} \sum_{i < j}^{\infty} a_{ij}^k |\phi_i\phi_j(t)\rangle_{-} \oplus \dots \quad (2.38)$$



where for a given k , only one of $a^k, a_i^k, a_{ij}^k, \dots$ is 1 and others are 0. The inner product of two states $\Phi_{k'}(t)$ and $\Phi_k(t)$ is by definition:[52, 53]

$$\begin{aligned} \langle \Phi_{k'}(t) | \Phi_k(t) \rangle &= \left(a^{k'} \right)^* a^k \langle 0 | 0 \rangle + \sum_{i=0}^{\infty} \sum_{j=0}^{\infty} \left(a_i^{k'} \right)^* a_j^k \langle \phi_i(t) | \phi_j(t) \rangle \\ &+ \sum_{i=0}^{\infty} \sum_{i < j}^{\infty} \sum_{l=0}^{\infty} \sum_{l < m}^{\infty} \left(a_{ij}^{k'} \right)^* a_{lm}^k \langle \phi_i\phi_j(t) |_{-} | \phi_l\phi_m(t) \rangle_{-} + \dots \end{aligned} \quad (2.39)$$

By the orthonormality of the basis for respective N -electron Hilbert space, this expression simplifies to:

$$\langle \Phi_{k'}(t) | \Phi_k(t) \rangle = a^{k'} a^k + \sum_{i=0}^{\infty} a_i^{k'} a_i^k + \sum_{i=0}^{\infty} \sum_{i < j}^{\infty} a_{ij}^{k'} a_{ij}^k + \dots \quad (2.40)$$

$$= \delta_{k'k} \quad (2.41)$$

Thus, the states $|\Phi_k(t)\rangle$ form an orthonormal basis for the Fock space.

As a concrete example, the state $|\Phi_3(t)\rangle$, which in the coordinate representation (excluding spin) is given by:

$$\Phi_3(\mathbf{r}_1, \mathbf{r}_2, t) = \frac{1}{\sqrt{2!}} (\phi_1(\mathbf{r}_1, t) \phi_2(\mathbf{r}_2, t) - \phi_2(\mathbf{r}_1, t) \phi_1(\mathbf{r}_2, t)) \quad (2.42)$$



By eq. (2.34) we have

$$\left(-\frac{1}{2} \nabla_{\mathbf{r}_1}^2 + v_s(\mathbf{r}_1, t_0) \right) \phi_1(\mathbf{r}_1, t_0) = \epsilon_1 \phi_1(\mathbf{r}_1, t_0) \quad (2.43)$$

$$\left(-\frac{1}{2} \nabla_{\mathbf{r}_2}^2 + v_s(\mathbf{r}_2, t_0) \right) \phi_1(\mathbf{r}_2, t_0) = \epsilon_1 \phi_1(\mathbf{r}_2, t_0) \quad (2.44)$$

$$\left(-\frac{1}{2} \nabla_{\mathbf{r}_1}^2 + v_s(\mathbf{r}_1, t_0) \right) \phi_2(\mathbf{r}_1, t_0) = \epsilon_2 \phi_2(\mathbf{r}_1, t_0) \quad (2.45)$$

$$\left(-\frac{1}{2} \nabla_{\mathbf{r}_2}^2 + v_s(\mathbf{r}_2, t_0) \right) \phi_2(\mathbf{r}_2, t_0) = \epsilon_2 \phi_2(\mathbf{r}_2, t_0) \quad (2.46)$$

By multiplying appropriate factors on both sides of each equation, we obtain the following equations:

$$\left(-\frac{1}{2} \nabla_{\mathbf{r}_1}^2 + v_s(\mathbf{r}_1, t_0) \right) \phi_1(\mathbf{r}_1, t_0) \phi_2(\mathbf{r}_2, t_0) = \epsilon_1 \phi_1(\mathbf{r}_1, t_0) \phi_2(\mathbf{r}_2, t_0) \quad (2.47)$$

$$\left(-\frac{1}{2} \nabla_{\mathbf{r}_2}^2 + v_s(\mathbf{r}_2, t_0) \right) \phi_2(\mathbf{r}_1, t_0) \phi_1(\mathbf{r}_2, t_0) = \epsilon_1 \phi_2(\mathbf{r}_1, t_0) \phi_1(\mathbf{r}_2, t_0) \quad (2.48)$$

$$\left(-\frac{1}{2} \nabla_{\mathbf{r}_1}^2 + v_s(\mathbf{r}_1, t_0) \right) \phi_2(\mathbf{r}_1, t_0) \phi_1(\mathbf{r}_2, t_0) = \epsilon_2 \phi_2(\mathbf{r}_1, t_0) \phi_1(\mathbf{r}_2, t_0) \quad (2.49)$$

$$\left(-\frac{1}{2} \nabla_{\mathbf{r}_2}^2 + v_s(\mathbf{r}_2, t_0) \right) \phi_1(\mathbf{r}_1, t_0) \phi_2(\mathbf{r}_2, t_0) = \epsilon_2 \phi_1(\mathbf{r}_1, t_0) \phi_2(\mathbf{r}_2, t_0) \quad (2.50)$$

$((2.47) + (2.50) - (2.49) - (2.48))$ multiplied by $\frac{1}{\sqrt{2!}}$, we obtain:

$$\left(-\frac{1}{2} \nabla_{\mathbf{r}_1}^2 + v_s(\mathbf{r}_1, t_0) - \frac{1}{2} \nabla_{\mathbf{r}_2}^2 + v_s(\mathbf{r}_2, t_0) \right) \Phi_3(\mathbf{r}_1, \mathbf{r}_2, t_0) = (\epsilon_1 + \epsilon_2) \Phi_3(\mathbf{r}_1, \mathbf{r}_2, t_0) \quad (2.51)$$

which corresponds to eq. (2.28) in the coordinate representation with $k = 3$. This equation gives us the energy of $|\Phi_3(t)\rangle$ as:

$$E_3 = \epsilon_1 + \epsilon_2 \quad (2.52)$$

The number of electrons of $|\Phi_3(t)\rangle$ is apparently $N_3 = 2$. Therefore, the state $|\Phi_3(t)\rangle$

initially possesses a definite energy E_3 and a definite number of electrons N_3 , and satisfies eq. (2.28). Similar arguments can be made for other values of k .

In summary, we have shown that the states $|\Phi_k(t)\rangle$ form a basis satisfying all the conditions specified in section 2.4, as we claimed.

For completeness, we further show the consistency between eqs. (2.31) and (2.35).

Starting with eq. (2.35):

$$i\frac{\partial}{\partial t}\phi_1(\mathbf{r}_1, t) = \left(-\frac{1}{2}\nabla_{\mathbf{r}_1}^2 + v_s(\mathbf{r}_1, t)\right)\phi_1(\mathbf{r}_1, t) \quad (2.53)$$

$$i\frac{\partial}{\partial t}\phi_1(\mathbf{r}_2, t) = \left(-\frac{1}{2}\nabla_{\mathbf{r}_2}^2 + v_s(\mathbf{r}_2, t)\right)\phi_1(\mathbf{r}_2, t) \quad (2.54)$$

$$i\frac{\partial}{\partial t}\phi_2(\mathbf{r}_1, t) = \left(-\frac{1}{2}\nabla_{\mathbf{r}_1}^2 + v_s(\mathbf{r}_1, t)\right)\phi_2(\mathbf{r}_1, t) \quad (2.55)$$

$$i\frac{\partial}{\partial t}\phi_2(\mathbf{r}_2, t) = \left(-\frac{1}{2}\nabla_{\mathbf{r}_2}^2 + v_s(\mathbf{r}_2, t)\right)\phi_2(\mathbf{r}_2, t) \quad (2.56)$$

By multiplying appropriate factors on both sides of each equation, we obtain:

$$i\phi_2(\mathbf{r}_2, t)\frac{\partial}{\partial t}\phi_1(\mathbf{r}_1, t) = \left(-\frac{1}{2}\nabla_{\mathbf{r}_1}^2 + v_s(\mathbf{r}_1, t)\right)\phi_1(\mathbf{r}_1, t)\phi_2(\mathbf{r}_2, t) \quad (2.57)$$

$$i\phi_2(\mathbf{r}_1, t)\frac{\partial}{\partial t}\phi_1(\mathbf{r}_2, t) = \left(-\frac{1}{2}\nabla_{\mathbf{r}_2}^2 + v_s(\mathbf{r}_2, t)\right)\phi_2(\mathbf{r}_1, t)\phi_1(\mathbf{r}_2, t) \quad (2.58)$$

$$i\phi_1(\mathbf{r}_2, t)\frac{\partial}{\partial t}\phi_2(\mathbf{r}_1, t) = \left(-\frac{1}{2}\nabla_{\mathbf{r}_1}^2 + v_s(\mathbf{r}_1, t)\right)\phi_2(\mathbf{r}_1, t)\phi_1(\mathbf{r}_2, t) \quad (2.59)$$

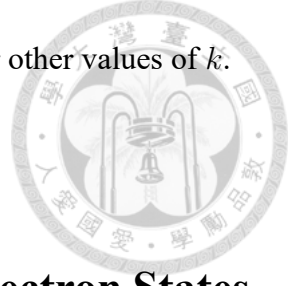
$$i\phi_1(\mathbf{r}_1, t)\frac{\partial}{\partial t}\phi_2(\mathbf{r}_2, t) = \left(-\frac{1}{2}\nabla_{\mathbf{r}_2}^2 + v_s(\mathbf{r}_2, t)\right)\phi_1(\mathbf{r}_1, t)\phi_2(\mathbf{r}_2, t) \quad (2.60)$$

$((2.57) + (2.60) - (2.59) - (2.58))$ multiplied by $\frac{1}{\sqrt{2!}}$, we obtain:

$$i\frac{\partial}{\partial t}\Phi_3(\mathbf{r}_1, \mathbf{r}_2, t) = \left(-\frac{1}{2}\nabla_{\mathbf{r}_1}^2 + v_s(\mathbf{r}_1, t) - \frac{1}{2}\nabla_{\mathbf{r}_2}^2 + v_s(\mathbf{r}_2, t)\right)\Phi_3(\mathbf{r}_1, \mathbf{r}_2, t) \quad (2.61)$$

This equation corresponds to eq. (2.31) in the coordinate representation with $k = 3$. There-

fore, the equations are consistent. Similar arguments can be made for other values of k .



2.6 Ensemble Average Evaluated by One-Electron States

As discussed in section 2.3, we here deduce the formulation of one-electron states from that of mixed states. Consider an operator \hat{O} [48]

$$\hat{O} = \bigoplus_{N=1}^{\infty} \hat{O}^N \quad (2.62)$$

where the operator \hat{O}^N is the sum of one-body operators \hat{o}_j acting on the electron j

$$\hat{O}^N = \sum_{j=1}^N \hat{o}_j \quad (2.63)$$

Note that eq. (2.62) implicitly introduces the zero operator $\hat{0}$.[53]

$$\hat{O} = \hat{0} \oplus \hat{O}^1 \oplus \hat{O}^2 \oplus \dots \quad (2.64)$$

We will demonstrate that the expectation value of \hat{O} for the TAO ensemble (ensemble average of \hat{O}) at any time t can be evaluated by one-electron states $|\phi_i(t)\rangle$ and the Fermi–Dirac function f_i [54, 55]

$$\left\langle \hat{O} \right\rangle_{\hat{\Gamma}_s}(t) = \sum_{i=1}^{\infty} f_i \langle \phi_i(t) | \hat{o} | \phi_i(t) \rangle \quad (2.65)$$

where it is recognized that the one-body operator \hat{o} and one-electron states $|\phi_i(t)\rangle$ live in the same one-electron Hilbert space. The Fermi–Dirac function is given by

$$f_i = \{1 + \exp[(\epsilon_i - \mu)/\theta]\}^{-1} \quad (2.4)$$

Alternatively, if we introduce the one-electron density operator $\hat{\gamma}_s(t)$ defined by

$$\hat{\gamma}_s(t) = \sum_{i=1}^{\infty} f_i |\phi_i(t)\rangle\langle\phi_i(t)| \quad (2.66)$$



then it can be shown that

$$\langle \hat{O} \rangle_{\hat{\Gamma}_s}(t) = \text{tr}(\hat{\gamma}_s(t)\hat{O}) \quad (2.67)$$

is equivalent to eq. (2.65).

Firstly, from standard textbooks,[8, 51, 56] we know the ensemble average of an operator \hat{O} for the TAO ensemble is given by the trace of the product of the density operator $\hat{\Gamma}_s(t)$ and the operator \hat{O}

$$\langle \hat{O} \rangle_{\hat{\Gamma}_s}(t) = \text{tr}(\hat{\Gamma}_s(t)\hat{O}) \quad (2.68)$$

Now, we introduce states $|\Phi_{k'}(t)\rangle$ which form a basis satisfying all conditions specified in section 2.4 ($|\Phi_0(t)\rangle = |0\rangle$ without loss of generality). The ensemble average of \hat{O} can be expressed as a sum over this basis

$$\langle \hat{O} \rangle_{\hat{\Gamma}_s}(t) = \sum_{k'=0}^{\infty} \langle \Phi_{k'}(t) | \hat{\Gamma}_s(t) \hat{O} | \Phi_{k'}(t) \rangle \quad (2.69)$$

Expanding the time-dependent mixed state $\hat{\Gamma}_s(t)$ by eq. (2.32) with the same basis $|\Phi_k(t)\rangle$, we get

$$\langle \hat{O} \rangle_{\hat{\Gamma}_s}(t) = \sum_{k=0}^{\infty} \sum_{k'=0}^{\infty} w_k \langle \Phi_{k'}(t) | \Phi_k(t) \rangle \langle \Phi_k(t) | \hat{O} | \Phi_{k'}(t) \rangle \quad (2.70)$$

By the orthonormality of the basis $|\Phi_k(t)\rangle$, we have

$$\langle \hat{O} \rangle_{\hat{\Gamma}_s}(t) = \sum_{k=0}^{\infty} w_k \langle \Phi_k(t) | \hat{O} | \Phi_k(t) \rangle \quad (2.71)$$

Since $\langle 0|\hat{0}|0\rangle = 0$, eq. (2.71) can be further simplified to

$$\left\langle \hat{O} \right\rangle_{\hat{\Gamma}_s}(t) = \sum_{k=1}^{\infty} w_k \langle \Phi_k(t) | \hat{O} | \Phi_k(t) \rangle \quad (2.72)$$



Finally, by eq. (2.63), we obtain

$$\left\langle \hat{O} \right\rangle_{\hat{\Gamma}_s}(t) = \sum_{k=1}^{\infty} w_k \sum_{j=1}^{N_k} \langle \Phi_k(t) | \hat{o}_j | \Phi_k(t) \rangle \quad (2.73)$$

Now, because the states $|\Phi_k(t)\rangle$ are anti-symmetrized such that electrons are indistinguishable, the N_k terms in eq. (2.73) equal, and the summation over j is equivalent to multiplying by N_k

$$\sum_{j=1}^{N_k} \langle \Phi_k(t) | \hat{o}_j | \Phi_k(t) \rangle = N_k \langle \Phi_k(t) | \hat{o}_j | \Phi_k(t) \rangle \quad (2.74)$$

The term $\langle \Phi_k(t) | \hat{o}_j | \Phi_k(t) \rangle$ can be expressed as

$$\langle \Phi_k(t) | \hat{o}_j | \Phi_k(t) \rangle = \sum_i \frac{(N_k - 1)!}{N_k!} \langle \phi_i^j(t) | \hat{o}_j | \phi_i^j(t) \rangle = \sum_i \frac{1}{N_k} \langle \phi_i(t) | \hat{o} | \phi_i(t) \rangle \quad (2.75)$$

where the summation is over all occurring one-electron states $|\phi_i^j(t)\rangle$ of the electron j , the term $N_k!$ is the coefficient introduced for anti-symmetrization, and the term $(N_k - 1)!$ is the number of terms relating to changing indices of the $(N_k - 1)$ electrons other than the electron j . In the last equality, the index j is dropped, and it is recognized that the one-body operator \hat{o} and one-electron states $|\phi_i(t)\rangle$ live in the same one-electron Hilbert space.

Starting from eqs. (2.73) to (2.75), we have

$$\langle \hat{O} \rangle_{\hat{\Gamma}_s}(t) = \sum_{k=1}^{\infty} w_k \sum_i \langle \phi_i(t) | \hat{o} | \phi_i(t) \rangle \quad (2.76)$$



Next, we introduce n_i^k , which is the occupation number of the orbital $\phi_i(\mathbf{r}, t)$ for the state $|\Phi_k(t)\rangle$. Apparently, the occupation numbers n_i^k are time-independent, and we have

$$\langle \hat{O} \rangle_{\hat{\Gamma}_s}(t) = \sum_{k=1}^{\infty} w_k \sum_{i=1}^{\infty} n_i^k \langle \phi_i(t) | \hat{o} | \phi_i(t) \rangle \quad (2.77)$$

The summation over i is now independent of k , so we can interchange the two summations and get

$$\langle \hat{O} \rangle_{\hat{\Gamma}_s}(t) = \sum_{i=1}^{\infty} \sum_{k=1}^{\infty} \langle \phi_i(t) | \hat{o} | \phi_i(t) \rangle w_k n_i^k \quad (2.78)$$

Also, the term $\langle \phi_i(t) | \hat{o} | \phi_i(t) \rangle$ is independent of k , so we can move it out of the summation over k and obtain

$$\langle \hat{O} \rangle_{\hat{\Gamma}_s}(t) = \sum_{i=1}^{\infty} \langle \phi_i(t) | \hat{o} | \phi_i(t) \rangle \sum_{k=1}^{\infty} w_k n_i^k \quad (2.79)$$

Because $n_i^0 = 0$ for all i , $\sum_{k=1}^{\infty} w_k n_i^k = \sum_{k=0}^{\infty} w_k n_i^k$ and we have

$$\langle \hat{O} \rangle_{\hat{\Gamma}_s}(t) = \sum_{i=1}^{\infty} \langle \phi_i(t) | \hat{o} | \phi_i(t) \rangle \sum_{k=0}^{\infty} w_k n_i^k \quad (2.80)$$

The summation over k is nothing but the mean occupation number $\langle n_i \rangle_{\hat{\Gamma}_s}$ of an orbital $\phi_i(\mathbf{r}, t)$. This can be shown by considering the corresponding operator \hat{n}_i such that

$$\hat{n}_i |\Phi_k(t)\rangle = n_i^k |\Phi_k(t)\rangle \quad (2.81)$$



By eq. (2.71), we have

$$\langle n_i \rangle_{\hat{\Gamma}_s}(t) = \sum_{k=0}^{\infty} w_k \langle \Phi_k(t) | \hat{n}_i | \Phi_k(t) \rangle = \sum_{k=0}^{\infty} w_k \langle \Phi_k(t) | n_i^k | \Phi_k(t) \rangle = \sum_{k=0}^{\infty} w_k n_i^k \quad (2.82)$$

On the left hand side, we drop the hat of \hat{n}_i which is a mere emphasis of the operator.

Because w_k and n_i^k are time-independent, so is the summation, and we can drop the time-dependence and obtain

$$\sum_{k=0}^{\infty} w_k n_i^k = \langle n_i \rangle_{\hat{\Gamma}_s} \quad (2.83)$$

Finally, because the TAO ensemble $\hat{\Gamma}_s(t)$ is initially a grand canonical ensemble, we have

$$\langle n_i \rangle_{\hat{\Gamma}_s} = \{1 + \exp[(\epsilon_i - \mu)/\theta]\}^{-1} \equiv f_i \quad (2.84)$$

which is the Fermi–Dirac function, with the derivation provided in standard textbooks.[56]

Combining eqs. (2.80), (2.83) and (2.84), we obtain eq. (2.65) as required.

To show that eq. (2.67) is equivalent to eq. (2.65), we start with eq. (2.67) and introduce one-electron states $|\phi_{i'}(t)\rangle$ as follows:

$$\langle \hat{O} \rangle_{\hat{\Gamma}_s}(t) = \sum_{i'=1}^{\infty} \langle \phi_{i'}(t) | \hat{\gamma}_s(t) \hat{o} | \phi_{i'}(t) \rangle \quad (2.85)$$

Next, we expand the one-electron density operator $\hat{\gamma}_s(t)$ by eq. (2.66) with the same basis

$|\phi_i(t)\rangle$:

$$\langle \hat{O} \rangle_{\hat{\Gamma}_s}(t) = \sum_{i=1}^{\infty} \sum_{i'=1}^{\infty} f_i \langle \phi_{i'}(t) | \phi_i(t) \rangle \langle \phi_i(t) | \hat{o} | \phi_{i'}(t) \rangle \quad (2.86)$$

By the orthonormality of the basis $|\phi_i(t)\rangle$, we get:

$$\langle \hat{O} \rangle_{\hat{\Gamma}_s}(t) = \sum_{i=1}^{\infty} f_i \langle \phi_i(t) | \hat{o} | \phi_i(t) \rangle \quad (2.65)$$

which is eq. (2.65) as required.



2.7 Expression of the RT-TAO Potential

To obtain the expression of the RT-TAO potential, we begin with the generalization of the RG theorems to ensembles, which allows the time-dependent mixed state $\hat{\Gamma}_s(t)$ to be written as a functional of the time-dependent density $n(\mathbf{r}, t)$ and the initial mixed state $\hat{\Gamma}_s(t_0)$.^[44] The equilibrium mixed state $\hat{\Gamma}_s(t_0)$ can be written as a functional of the equilibrium density $n_0(\mathbf{r}) = n(\mathbf{r}, t_0)$ by the generalization of the HK theorems to grand canonical ensembles.^[20] Thus, the initial mixed state dependence can be absorbed in $n(\mathbf{r}, t)$ and obtain

$$\hat{\Gamma}_s(t) = \hat{\Gamma}_s[n](t) \quad (2.87)$$

Next, we define the action integral $A[n]$ for the ensemble $\hat{\Gamma}[n](t)$ (without specification of interaction) as provided by Li^[45]:

$$A[n] = \int_{t_0}^{t_1} dt \operatorname{tr} \left(\hat{\Gamma}[n](t) \left(i \frac{\partial}{\partial t} - \hat{H}(t) \right) \right) \quad (2.88)$$

where $\hat{H}(t)$ is the time-dependent Hamiltonian. The action integral gives a stationary point if the input density is the exact time-dependent density $n(\mathbf{r}, t)$ associated with the Hamiltonian $\hat{H}(t)$. That is, the exact time-dependent density $n(\mathbf{r}, t)$ satisfies the Euler equation:

$$\frac{\delta A[n]}{\delta n(\mathbf{r}, t)} = 0 \quad (2.89)$$

It is understood that ensembles with all kinds of interaction, including the TAO ensemble $\hat{\Gamma}_s[n](t)$ and $\hat{\Gamma}_W[n](t)$ (see below), lead to similar arguments.

For the true interacting system, the Hamiltonian is given by

$$\hat{H}^{N_{\text{el}}}(t) = \hat{T}^{N_{\text{el}}} + \hat{V}^{N_{\text{el}}}(t) + \hat{W}^{N_{\text{el}}} \quad (2.90)$$



where $\hat{T}^{N_{\text{el}}}$ is the kinetic energy operator

$$\hat{T}^{N_{\text{el}}} = \sum_{j=1}^{N_{\text{el}}} \left(-\frac{1}{2} \nabla_{\mathbf{r}_j}^2 \right) \quad (2.24)$$

$\hat{V}^{N_{\text{el}}}(t)$ is the external potential

$$\hat{V}^{N_{\text{el}}}(t) = \sum_{j=1}^{N_{\text{el}}} v(\mathbf{r}_j, t) \quad (2.91)$$

and $\hat{W}^{N_{\text{el}}}$ is the electron-electron interaction term

$$\hat{W}^{N_{\text{el}}} = \frac{1}{2} \sum_{j=1}^{N_{\text{el}}} \sum_{j'=1, j' \neq j}^{N_{\text{el}}} \frac{1}{\|\mathbf{r}_j - \mathbf{r}_{j'}\|} \quad (2.92)$$

The ensemble $\hat{\Gamma}_W[n](t)$ is defined as

$$\hat{\Gamma}_W[n](t) = |\Psi[n](t)\rangle\langle\Psi[n](t)| \quad (2.93)$$

by eq. (2.21). The action integral eq. (2.88) for $\hat{\Gamma}_W[n](t)$ can be rewritten as

$$A_W[n] = \int_{t_0}^{t_1} dt \text{tr} \left(\hat{\Gamma}_W[n](t) \left(i \frac{\partial}{\partial t} - \hat{H}^{N_{\text{el}}}(t) \right) \right) \quad (2.94)$$

or¹

$$A_W[n] = \int_{t_0}^{t_1} dt \langle \Psi[n](t) | \left(i \frac{\partial}{\partial t} - \hat{T}^{N_{\text{el}}} \right) | \Psi[n](t) \rangle - \int_{t_0}^{t_1} dt \int d\mathbf{r} v(\mathbf{r}, t) n(\mathbf{r}, t) - \int_{t_0}^{t_1} dt \langle \Psi[n](t) | \hat{W}^{N_{\text{el}}} | \Psi[n](t) \rangle \quad (2.95)$$

The Euler equation eq. (2.89) for $\hat{\Gamma}_W[n](t)$ becomes

$$\frac{\delta}{\delta n(\mathbf{r}, t)} \left(\int_{t_0}^{t_1} dt \langle \Psi[n](t) | \left(i \frac{\partial}{\partial t} - \hat{T}^{N_{\text{el}}} \right) | \Psi[n](t) \rangle - v(\mathbf{r}, t) \right. \\ \left. - \frac{\delta}{\delta n(\mathbf{r}, t)} \left(\int_{t_0}^{t_1} dt \langle \Psi[n](t) | \hat{W}^{N_{\text{el}}} | \Psi[n](t) \rangle \right) \right) = 0 \quad (2.96)$$

On the other hand, the Hamiltonian of the fictitious non-interacting ensemble is provided by eq. (2.22), and the ensemble is given in eq. (2.87). The action integral eq. (2.88) for $\hat{\Gamma}_s[n](t)$ can be rewritten as

$$A_s[n] = \int_{t_0}^{t_1} dt \text{tr} \left(\hat{\Gamma}_s[n](t) \left(i \frac{\partial}{\partial t} - \hat{H}_s(t) \right) \right) \quad (2.97)$$

or¹

$$A_s[n] = \int_{t_0}^{t_1} dt \text{tr} \left(\hat{\Gamma}_s[n](t) \left(i \frac{\partial}{\partial t} - \hat{T}_s \right) \right) - \int_{t_0}^{t_1} dt \int d\mathbf{r} v_s(\mathbf{r}, t) n(\mathbf{r}, t) \quad (2.98)$$

where \hat{T}_s is the kinetic energy operator defined as[48]

$$\hat{T}_s = \bigoplus_{N=1}^{\infty} \hat{T}^N \quad (2.99)$$

¹See section 2.8.

The Euler equation eq. (2.89) for $\hat{\Gamma}_s[n](t)$ becomes

$$\frac{\delta}{\delta n(\mathbf{r}, t)} \left(\int_{t_0}^{t_1} dt \operatorname{tr} \left(\hat{\Gamma}_s[n](t) \left(i \frac{\partial}{\partial t} - \hat{T}_s \right) \right) \right) - v_s(\mathbf{r}, t) = 0 \quad (2.100)$$



Observe that

$$\frac{\delta}{\delta n(\mathbf{r}, t)} \left(\frac{1}{2} \int_{t_0}^{t_1} dt \int d\mathbf{r} \int d\mathbf{r}' \frac{n(\mathbf{r}, t)n(\mathbf{r}', t)}{\|\mathbf{r} - \mathbf{r}'\|} \right) = \int d\mathbf{r}' \frac{n(\mathbf{r}', t)}{\|\mathbf{r} - \mathbf{r}'\|} \quad (2.101)$$

(2.96) – (2.100) + (2.101), we get

$$\begin{aligned} v_s(\mathbf{r}, t) &= v(\mathbf{r}, t) + \int d\mathbf{r}' \frac{n(\mathbf{r}', t)}{\|\mathbf{r} - \mathbf{r}'\|} \\ &+ \frac{\delta}{\delta n(\mathbf{r}, t)} \left(\int_{t_0}^{t_1} dt \langle \Psi[n](t) | \hat{W}^{N_{\text{el}}} | \Psi[n](t) \rangle - \frac{1}{2} \int_{t_0}^{t_1} dt \int d\mathbf{r} \int d\mathbf{r}' \frac{n(\mathbf{r}, t)n(\mathbf{r}', t)}{\|\mathbf{r} - \mathbf{r}'\|} \right. \\ &\quad \left. + \int_{t_0}^{t_1} dt \operatorname{tr} \left(\hat{\Gamma}_s[n](t) \left(i \frac{\partial}{\partial t} - \hat{T}_s \right) \right) - \int_{t_0}^{t_1} dt \langle \Psi[n](t) | \left(i \frac{\partial}{\partial t} - \hat{T}^{N_{\text{el}}} \right) | \Psi[n](t) \rangle \right) \end{aligned} \quad (2.102)$$

Now follow the definition of $v_{\text{HXC}\theta}[n](\mathbf{r}, t)$ in eq. (2.18), we get

$$v_{\text{HXC}\theta}[n](\mathbf{r}, t) = \int d\mathbf{r}' \frac{n(\mathbf{r}', t)}{\|\mathbf{r} - \mathbf{r}'\|} + \frac{\delta A_{\text{XC}\theta}[n]}{\delta n(\mathbf{r}, t)} \quad (2.103)$$

where

$$\begin{aligned} A_{\text{XC}\theta}[n] &= \int_{t_0}^{t_1} dt \langle \Psi[n](t) | \hat{W}^{N_{\text{el}}} | \Psi[n](t) \rangle - \frac{1}{2} \int_{t_0}^{t_1} dt \int d\mathbf{r} \int d\mathbf{r}' \frac{n(\mathbf{r}, t)n(\mathbf{r}', t)}{\|\mathbf{r} - \mathbf{r}'\|} \\ &+ \int_{t_0}^{t_1} dt \operatorname{tr} \left(\hat{\Gamma}_s[n](t) \left(i \frac{\partial}{\partial t} - \hat{T}_s \right) \right) - \int_{t_0}^{t_1} dt \langle \Psi[n](t) | \left(i \frac{\partial}{\partial t} - \hat{T}^{N_{\text{el}}} \right) | \Psi[n](t) \rangle \end{aligned} \quad (2.104)$$

Note the initial state dependence $|\Psi(t_0)\rangle$ and $\hat{\Gamma}_s(t_0)$ have been absorbed in the time-dependent density $n(\mathbf{r}, t)$ by eqs. (2.21) and (2.87), similar to RT-TD-DFT.[8]



2.8 Some Details of Derivations

First, we want to write down the expression of the time-dependent density $n(\mathbf{r}, t)$.

For the true interacting system, the operator for the time-dependent density $\hat{n}(\mathbf{r})$ is[57]

$$\hat{n}(\mathbf{r}) = \sum_{j=1}^{N_{\text{el}}} \delta(\mathbf{r} - \mathbf{r}_j) \quad (2.105)$$

so the time-dependent density $n(\mathbf{r}, t)$ is

$$n(\mathbf{r}, t) = \langle \Psi(t) | \hat{n}(\mathbf{r}) | \Psi(t) \rangle \quad (2.106)$$

$$\begin{aligned} &= \int d\mathbf{r}_1 d\mathbf{r}_2 \cdots d\mathbf{r}_{N_{\text{el}}} \langle \Psi(t) | \mathbf{r}_1, \mathbf{r}_2, \dots, \mathbf{r}_{N_{\text{el}}} \rangle \langle \mathbf{r}_1, \mathbf{r}_2, \dots, \mathbf{r}_{N_{\text{el}}} | \hat{n}(\mathbf{r}) | \Psi(t) \rangle \quad (2.107) \\ &= \int d\mathbf{r}_1 d\mathbf{r}_2 \cdots d\mathbf{r}_{N_{\text{el}}} \Psi^*(\mathbf{r}_1, \mathbf{r}_2, \dots, \mathbf{r}_{N_{\text{el}}}, t) \sum_{j=1}^{N_{\text{el}}} \delta(\mathbf{r} - \mathbf{r}_j) \Psi(\mathbf{r}_1, \mathbf{r}_2, \dots, \mathbf{r}_{N_{\text{el}}}, t) \end{aligned}$$

$$(2.108)$$

$$= N_{\text{el}} \int d\mathbf{r}_2 \cdots d\mathbf{r}_{N_{\text{el}}} \Psi^*(\mathbf{r}, \mathbf{r}_2, \dots, \mathbf{r}_{N_{\text{el}}}, t) \Psi(\mathbf{r}, \mathbf{r}_2, \dots, \mathbf{r}_{N_{\text{el}}}, t) \quad (2.109)$$

which is a form one may be familiar with.

For the fictitious non-interacting ensemble, the operator for the time-dependent density $\hat{n}_s(\mathbf{r})$ can be easily generalized as[48]

$$\hat{n}_s(\mathbf{r}) = \bigoplus_{N=1}^{\infty} \hat{n}_s^N(\mathbf{r}) \quad (2.110)$$

where

$$\hat{n}_s^N(\mathbf{r}) = \sum_{j=1}^N \delta(\mathbf{r} - \mathbf{r}_j) \quad (2.111)$$

so by eq. (2.65), the time-dependent density $n(\mathbf{r}, t)$ is

$$n(\mathbf{r}, t) = \sum_{i=1}^{\infty} f_i \int d\mathbf{r}' \langle \phi_i(t) | \mathbf{r}' \rangle \langle \mathbf{r}' | \delta(\mathbf{r} - \mathbf{r}') | \phi_i(t) \rangle \quad (2.112)$$

$$= \sum_{i=1}^{\infty} f_i \int d\mathbf{r}' \phi_i^*(\mathbf{r}', t) \delta(\mathbf{r} - \mathbf{r}') \phi_i(\mathbf{r}', t) \quad (2.113)$$

$$= \sum_{i=1}^{\infty} f_i \phi_i^*(\mathbf{r}, t) \phi_i(\mathbf{r}, t) \quad (2.114)$$



Now the term in eq. (2.94) becomes

$$\int_{t_0}^{t_1} dt \text{tr} \left(\hat{\Gamma}_W[n](t) \hat{V}^{N_{\text{el}}}(t) \right) \quad (2.115)$$

$$= \int_{t_0}^{t_1} dt \langle \Psi[n](t) | \hat{V}^{N_{\text{el}}}(t) | \Psi[n](t) \rangle \quad (2.116)$$

$$= \int_{t_0}^{t_1} dt \int d\mathbf{r}_1 d\mathbf{r}_2 \cdots d\mathbf{r}_{N_{\text{el}}} \langle \Psi[n](t) | \mathbf{r}_1, \mathbf{r}_2, \dots, \mathbf{r}_{N_{\text{el}}} \rangle \langle \mathbf{r}_1, \mathbf{r}_2, \dots, \mathbf{r}_{N_{\text{el}}} | \hat{V}^{N_{\text{el}}}(t) | \Psi[n](t) \rangle \quad (2.117)$$

$$= \int_{t_0}^{t_1} dt \int d\mathbf{r}_1 d\mathbf{r}_2 \cdots d\mathbf{r}_{N_{\text{el}}} \Psi^*(\mathbf{r}_1, \mathbf{r}_2, \dots, \mathbf{r}_{N_{\text{el}}}, t) \sum_{j=1}^{N_{\text{el}}} v(\mathbf{r}_j, t) \Psi(\mathbf{r}_1, \mathbf{r}_2, \dots, \mathbf{r}_{N_{\text{el}}}, t) \quad (2.118)$$

$$= \int_{t_0}^{t_1} dt \int d\mathbf{r}_1 v(\mathbf{r}_1, t) N_{\text{el}} \int d\mathbf{r}_2 \cdots d\mathbf{r}_{N_{\text{el}}} \Psi^*(\mathbf{r}_1, \mathbf{r}_2, \dots, \mathbf{r}_{N_{\text{el}}}, t) \Psi(\mathbf{r}_1, \mathbf{r}_2, \dots, \mathbf{r}_{N_{\text{el}}}, t) \quad (2.119)$$

$$= \int_{t_0}^{t_1} dt \int d\mathbf{r}_1 v(\mathbf{r}_1, t) n(\mathbf{r}_1, t) \quad (2.120)$$

$$= \int_{t_0}^{t_1} dt \int d\mathbf{r} v(\mathbf{r}, t) n(\mathbf{r}, t) \quad (2.121)$$

In eq. (2.117), an identity operator $\hat{I} = \int d\mathbf{r}_1 d\mathbf{r}_2 \cdots d\mathbf{r}_{N_{\text{el}}} |\mathbf{r}_1, \mathbf{r}_2, \dots, \mathbf{r}_{N_{\text{el}}} \rangle \langle \mathbf{r}_1, \mathbf{r}_2, \dots, \mathbf{r}_{N_{\text{el}}} |$ is inserted. In eq. (2.119), $n(\mathbf{r}_1, t)$ is identified with eq. (2.109).



The term in eq. (2.97) becomes

$$\int_{t_0}^{t_1} dt \operatorname{tr} \left(\hat{\Gamma}_s[n](t) \hat{V}_s(t) \right) = \int_{t_0}^{t_1} dt \left\langle \hat{V}_s(t) \right\rangle_{\hat{\Gamma}_s}(t) \quad (2.123)$$

$$= \int_{t_0}^{t_1} dt \sum_{i=1}^{\infty} f_i \langle \phi_i(t) | \hat{v}_s(t) | \phi_i(t) \rangle \quad (2.124)$$

$$= \int_{t_0}^{t_1} dt \sum_{i=1}^{\infty} f_i \int d\mathbf{r} \langle \phi_i(t) | \mathbf{r} \rangle \langle \mathbf{r} | \hat{v}_s(t) | \phi_i(t) \rangle \quad (2.125)$$

$$= \int_{t_0}^{t_1} dt \sum_{i=1}^{\infty} f_i \int d\mathbf{r} \phi_i^*(\mathbf{r}, t) v_s(\mathbf{r}, t) \phi_i(\mathbf{r}, t) \quad (2.126)$$

$$= \int_{t_0}^{t_1} dt \int d\mathbf{r} v_s(\mathbf{r}, t) \sum_{i=1}^{\infty} f_i \phi_i^*(\mathbf{r}, t) \phi_i(\mathbf{r}, t) \quad (2.127)$$

$$= \int_{t_0}^{t_1} dt \int d\mathbf{r} v_s(\mathbf{r}, t) n(\mathbf{r}, t) \quad (2.128)$$

where[48]

$$\hat{V}_s(t) = \bigoplus_{N=1}^{\infty} \hat{V}_s^N(t) \quad (2.129)$$

We use eq. (2.68) to get eq. (2.123), and use eq. (2.65) to get eq. (2.124). In eq. (2.125), an identity operator $\hat{I} = \int d\mathbf{r} |\mathbf{r}\rangle\langle\mathbf{r}|$ is inserted. In eq. (2.127), $n(\mathbf{r}, t)$ is identified with eq. (2.114).

2.9 Approximations for the HXC θ Potential

Let $n : (\mathbf{r}, t) \mapsto n(\mathbf{r}, t)$ be the mapping taking (\mathbf{r}, t) to the time-dependent density $n(\mathbf{r}, t)$, $n_{t'} : \mathbf{r} \mapsto n(\mathbf{r}, t')$ be the collection of mappings taking \mathbf{r} to the density $n(\mathbf{r}, t')$, and $n_0 : \mathbf{r} \mapsto n_0(\mathbf{r})$ be the mapping taking \mathbf{r} to the ground-state density $n_0(\mathbf{r})$. Recall in ground-state TAO-DFT, similar to eq. (2.18), the static HXC θ potential $v_{\text{HXC}\theta}^0[n_0](\mathbf{r})$ is

defined by

$$v_{\text{HXC}\theta}^0[n_0](\mathbf{r}) \equiv v_s(\mathbf{r}) - v(\mathbf{r}) \quad (2.130)$$



which may be approximated by LDA,[2] GGA,[3] and hybrid functionals,[4, 24] etc. Here

$v_{\text{HXC}\theta}^0 : (n_0, \mathbf{r}) \mapsto v_{\text{HXC}\theta}^0[n_0](\mathbf{r})$ denotes the mapping taking (n_0, \mathbf{r}) to the static HXC θ potential $v_{\text{HXC}\theta}^0[n_0](\mathbf{r})$.

RT-TAO is a formally exact theory, with the inexactness arising from the unknown and necessarily approximated $v_{\text{HXC}\theta}[n](\mathbf{r}, t)$ or $A_{\text{XC}\theta}[n]$ in eqs. (2.103) and (2.104). $v_{\text{HXC}\theta} : (n, \mathbf{r}, t) \mapsto v_{\text{HXC}\theta}[n](\mathbf{r}, t)$ denotes the mapping taking (n, \mathbf{r}, t) to $v_{\text{HXC}\theta}[n](\mathbf{r}, t)$. A possible option is the adiabatic approximation,[8] defined by blindly plugging in n_t rather than n_0 in $v_{\text{HXC}\theta}^0$

$$v_{\text{HXC}\theta}^{\text{adia}} : (n, \mathbf{r}, t) \mapsto v_{\text{HXC}\theta}^0[n_t](\mathbf{r}) \quad (2.131)$$

This means we ignore the whole memory effect and assume the HXC θ potential at time t can be well approximated by the instantaneous density n_t . Combine this with LDA as an example

$$v_{\text{HXC}\theta}^{\text{adia,LDA}} : (n, \mathbf{r}, t) \mapsto v_{\text{HXC}\theta}^{0,\text{LDA}}[n_t](\mathbf{r}) \quad (2.132)$$

We will refer to this as ALDA.

2.10 Practical Scheme of RT-TAO

For spin-restricted formulation:

1. Choose a value for θ and conduct ground-state TAO-DFT in section 2.1. We would end up with occupation numbers f_i , TAO orbitals $\phi_i(\mathbf{r}) = \phi_i(\mathbf{r}, t_0)$, and ground-state density $n_0(\mathbf{r}) = n(\mathbf{r}, t_0)$.

2. Construct the RT-TAO potential $v_s(\mathbf{r}, t_0)$ by

$$v_s(\mathbf{r}, t_0) = v(\mathbf{r}, t_0) + v_{\text{HXC}\theta}[n](\mathbf{r}, t_0) \quad (2.19)$$



where $v(\mathbf{r}, t_0)$ is the time-dependent external potential at $t = t_0$, and $v_{\text{HXC}\theta}[n](\mathbf{r}, t_0)$ is the HXC θ potential at $t = t_0$. $v_{\text{HXC}\theta}[n](\mathbf{r}, t_0)$ may need approximations as discussed in section 2.9.

3. With initial TAO orbitals $\phi_i(\mathbf{r}, t_0)$, solve

$$i \frac{\partial}{\partial t} \phi_i(\mathbf{r}, t) = \hat{h}_s(t) \phi_i(\mathbf{r}, t) \quad (2.35)$$

for time-dependent TAO orbitals $\phi_i(\mathbf{r}, t)$, where $\hat{h}_s(t)$ is the one-electron Hamiltonian

$$\hat{h}_s(t) = -\frac{1}{2} \nabla_{\mathbf{r}}^2 + v_s(\mathbf{r}, t) \quad (2.33)$$

Because $\hat{h}_s(t)$ depends on time-dependent TAO orbitals $\phi_i(\mathbf{r}, t)$, in practice, we need to discretize time and adopt specific propagator algorithms, such as the modified mid-point unitary transformation (MMUT) method as in TDKS.[58] Let Δt be the time step, we would end up with $\phi_i(\mathbf{r}, t_0 + \Delta t)$.

4. Obtain $n(\mathbf{r}, t_0 + \Delta t)$ by

$$n(\mathbf{r}, t + \Delta t) = \sum_{i=1}^{\infty} f_i \phi_i^*(\mathbf{r}, t + \Delta t) \phi_i(\mathbf{r}, t + \Delta t) \quad (2.114)$$

5. Repeat step 2 to 4 with incremental t until the desired final time t_1 .

6. The whole history $n(\mathbf{r}, t)$ is the predicted time-dependent density in the interacting

system.

For spin-unrestricted formulation, the procedure is similar to the spin-restricted case with a few modifications:

1. Choose a value for θ and conduct ground-state TAO-DFT in section 2.1. We would end up with occupation numbers f_i^σ , spin TAO orbitals $\phi_i^\sigma(\mathbf{r}) = \phi_i^\sigma(\mathbf{r}, t_0)$, spin densities $n_0^\sigma(\mathbf{r}) = n^\sigma(\mathbf{r}, t_0)$, and ground-state density $n_0(\mathbf{r}) = n(\mathbf{r}, t_0)$, where $\sigma = \alpha$ or β .
2. Construct the RT-TAO potential $v_s^\sigma(\mathbf{r}, t_0)$ by

$$v_s^\sigma(\mathbf{r}, t_0) = v(\mathbf{r}, t_0) + v_{\text{HXC}\theta}^\sigma[n^\alpha, n^\beta](\mathbf{r}, t_0) \quad (2.133)$$

where $v(\mathbf{r}, t_0)$ is the time-dependent external potential at $t = t_0$, and $v_{\text{HXC}\theta}^\sigma$ is the HXC θ potential at $t = t_0$. $v_{\text{HXC}\theta}^\sigma$ may need approximations as discussed in section 2.9. The adiabatic approximation[8]

$$v_{\text{HXC}\theta}^{\sigma, \text{adia}} : (n^\alpha, n^\beta, \mathbf{r}, t) \mapsto v_{\text{HXC}\theta}^{\sigma, 0}[n_t^\alpha, n_t^\beta](\mathbf{r}) \quad (2.134)$$

or the adiabatic approximation combined with LDA as an example

$$v_{\text{HXC}\theta}^{\sigma, \text{adia,LDA}} : (n^\alpha, n^\beta, \mathbf{r}, t) \mapsto v_{\text{HXC}\theta}^{\sigma, 0, \text{LDA}}[n_t^\alpha, n_t^\beta](\mathbf{r}) \quad (2.135)$$

We will refer to this as ALDA.

3. With initial spin TAO orbitals $\phi_i^\sigma(\mathbf{r}, t_0)$, solve

$$i \frac{\partial}{\partial t} \phi_i^\sigma(\mathbf{r}, t) = \hat{h}_s^\sigma(t) \phi_i^\sigma(\mathbf{r}, t) \quad (2.136)$$

for time-dependent spin TAO orbitals $\phi_i^\sigma(\mathbf{r}, t)$, in which $\hat{h}_s^\sigma(t)$ is the one-electron Hamiltonian

$$\hat{h}_s^\sigma(t) = -\frac{1}{2}\nabla_{\mathbf{r}}^2 + v_s^\sigma(\mathbf{r}, t) \quad (2.137)$$

Because $\hat{h}_s^\sigma(t)$ depends on time-dependent spin TAO orbitals $\phi_i^\alpha(\mathbf{r}, t)$ and $\phi_i^\beta(\mathbf{r}, t)$, in practice, we need to discretize time and adopt specific propagator algorithms, such as the modified mid-point unitary transformation (MMUT) method as in TDKS.[58]

Let Δt be the time step, we would end up with $\phi_i^\sigma(\mathbf{r}, t_0 + \Delta t)$.

4. Obtain $n^\sigma(\mathbf{r}, t_0 + \Delta t)$ by

$$n^\sigma(\mathbf{r}, t + \Delta t) = \sum_{i=1}^{\infty} f_i^\sigma \phi_i^{\sigma*}(\mathbf{r}, t + \Delta t) \phi_i^\sigma(\mathbf{r}, t + \Delta t) \quad (2.138)$$

and $n(\mathbf{r}, t + \Delta t)$ by

$$n(\mathbf{r}, t + \Delta t) = n^\alpha(\mathbf{r}, t + \Delta t) + n^\beta(\mathbf{r}, t + \Delta t) \quad (2.139)$$

5. Repeat step 2 to 4 with incremental t until the desired final time t_1 .

6. The whole history $n(\mathbf{r}, t)$ is the predicted time-dependent density in the interacting system.





Chapter 3 Results

3.1 High Harmonic Generation

High harmonic generation (HHG) is a non-linear phenomenon falling outside the scope of LR theory. When an intense laser hits a suitable target, photons at frequencies that are integer multiples (high harmonic) of the incoming laser are produced.

This process is typically understood with the semi-classical three-step model.[59, 60] First is the tunneling ionization of an electron. Second are the acceleration and reacceleration of the electron away and back to the nucleus by the laser field. Third is the recombination of the electron with the nucleus, with an emission of a photon at a frequency that is equal to the kinetic energy of the electron minus the ionization potential.

The spectrum of HHG typically starts with a few harmonics decreasing in intensity, as expected. What surprises is that they are followed by a plateau of harmonics which are nearly constant in intensity. The plateau extends up to a cut-off frequency, which is determined by the ponderomotive energy (the energy gained by an electron as it oscillates in the laser field) and the ionization potential of the electrons in the laser field, and abruptly decreases in intensity.

To assess RT-TAO, HHG is chosen for three reasons. Firstly, LR-TD-DFT and TD-

TAO are unable to describe HHG, which highlights the importance of real-time theory as TDKS or RT-TAO. Secondly, the application of TDKS to HHG[5] serves as a reference and justifies the application of RT-TAO to HHG due to their similarities. Thirdly, the HHG spectrum is directly obtainable from the time-dependent density.

The HHG spectrum $H(\omega)$ in the dipole acceleration form is calculated by[8, 61]

$$H(\omega) = \sum_{k=x,y,z} \frac{1}{2\pi} \left| \int_{t_0}^{t_1} \frac{d^2 \mu_k(t)}{dt^2} w(t) e^{-i\omega t} dt \right|^2 \quad (3.1)$$

where $w(t)$ is the window function and $\mu_k(t)$ is the induced dipole moment along the electric field polarization \hat{k} (the minus sign accounts for the negative charge)[8]

$$\mu_k(t) = - \int k n(\mathbf{r}, t) d\mathbf{r} \quad (3.2)$$

For our case, the electric field polarization \hat{k} is along \hat{z} , so $\mu_x(t) = \mu_y(t) = 0$ and eq. (3.1) becomes

$$H(\omega) = \frac{1}{2\pi} \left| \int_{t_0}^{t_1} \frac{d^2 \mu_z(t)}{dt^2} w(t) e^{-i\omega t} dt \right|^2 \quad (3.3)$$

The window function $w(t)$ is taken to be the Hamming window

$$w(t) = 0.54 - 0.46 \cos\left(\frac{2\pi t}{t_1 - t_0}\right) \quad (3.4)$$

The results without applications of the window function are provided in appendix B for reference. Finally, the harmonic order is given by

$$\text{Harmonic order} = \omega/\omega_0 \quad (3.5)$$

where $\omega_0 = 1.5498 \text{ eV}$ is the fundamental frequency provided in section 3.3.



3.2 Time-Dependent Observables

Apart from the apparent time-dependent density $n(\mathbf{r}, t)$ and the induced dipole moments $\mu_k(t)$ (eq. (3.2)), there is another time-dependent observable directly obtainable from the time-dependent density $n(\mathbf{r}, t)$. That is the number of bound electrons $N_{\text{bound}}(t)$, given by[8]

$$N_{\text{bound}}(t) = \int d\mathbf{r} n(\mathbf{r}, t) \quad (3.6)$$

or equivalently the trace of the density matrix.[58] Here, the subscript “bound” is emphasized for the possible introduction of the complex absorbing potential (CAP), with which $N_{\text{bound}}(t)$ may decrease with time to simulate ionization.[8]

3.3 Computational Details

We implement RT-TAO on the fundation of the new TDKS module[5] (for RT-TD-DFT calculations) in the development version of Q-CHEM v. 5.4.[62]

The d-aug-cc-pVTZ[63–65] basis set is chosen. While ghost atom functions may be necessary to finely describe the high harmonics,[66] in this work, we focus on the improvement of broken symmetry between spin-restricted and spin-unrestricted formulations and adopt the pure standard d-aug-cc-pVTZ basis set. High-quality (99, 590)[67] integration grids are adopted in all calculations. As the first application of RT-TAO, local density approximation (LDA) XC-functionals (Slater[68] and PW92[69]) and LDA version of the E_θ functional[2] are employed. Applications of RT-TAO with other functionals are reserved for future works.

Under the conditions of the wavelength $\lambda \approx 800 \text{ nm}$ and the intensity $I \approx 1 \times 10^{14} \text{ W/cm}^2$, the dipole approximation is valid.[70] By the dipole approximation, the vector potential $\mathbf{A}(\mathbf{r}, t) \approx \mathbf{A}(t)$ and the magnetic field $\mathbf{B}(\mathbf{r}, t) = \nabla \times \mathbf{A}(\mathbf{r}, t) \approx \nabla \times \mathbf{A}(t) = 0$. Thus we may conduct a \cos^2 -shaped impulse with the electric field $\mathbf{E}(\mathbf{r}, t) = \mathbf{E}(t)$ along the z -axis (fig. 3.1) to mimic the common Ti:sapphire laser[66]

$$\mathbf{E}(t) = A_0 \cos^2 \left[\frac{\pi}{2\sigma_p} (\sigma_p - t) \right] \cos[\omega_0(t - \sigma_p)] \hat{z} \quad (3.7)$$

The amplitude $A_0 = 0.0534 \text{ a.u.}$ (the intensity $I = \frac{1}{2}\epsilon_0 c A_0^2 \approx 1 \times 10^{14} \text{ W/cm}^2$), $\sigma_p = 500 \text{ a.u.} \approx 12.1 \text{ fs}$ (the total pulse width $2\sigma_p = 1000 \text{ a.u.} \approx 24.1 \text{ fs}$ and the peak at 500 a.u. $\approx 12.1 \text{ fs}$), and the fundamental frequency $\omega_0 = 1.5498 \text{ eV}$ (the wavelength $\lambda \approx 800 \text{ nm}$). The resulting external potential of the laser $v_{\text{laser}}(\mathbf{r}, t)$ is (the origin is taken as the reference point)

$$v_{\text{laser}}(\mathbf{r}, t) = -\mathbf{r} \cdot \mathbf{E}(t) \quad (3.8)$$

or

$$v_{\text{laser}}(\mathbf{r}, t) = z \cdot A_0 \cos^2 \left[\frac{\pi}{2\sigma_p} (\sigma_p - t) \right] \cos[\omega_0(t - \sigma_p)] \quad (3.9)$$

In particular, eq. (3.9) is the equation used in our practical calculations.

To simulate electron ionization and to remove artificial reflections associated with the finite extent of the Gaussian basis, the complex absorbing potential (CAP) is introduced.[71] The CAP around the atom k positioned at \mathbf{R}_k is atom-centered-spherical, with

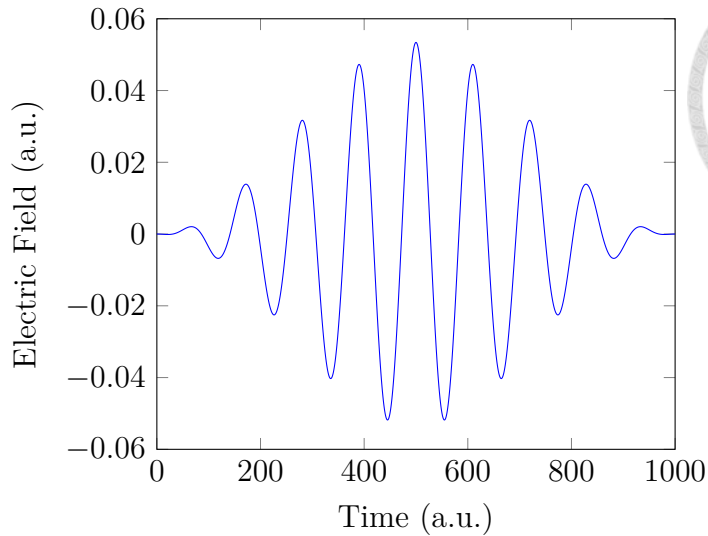


Figure 3.1: Electric field of the impulse.

value $f_k^{\text{CAP}}(\mathbf{r})$ at point \mathbf{r} , in a.u.

$$f_k^{\text{CAP}}(\mathbf{r}) = \begin{cases} 0, & \text{for } \|\mathbf{r} - \mathbf{R}_k\| < r_0 \\ \eta(\|\mathbf{r} - \mathbf{R}_k\| - r_0)^2, & \text{for } r_0 \leq \|\mathbf{r} - \mathbf{R}_k\| < r_0 + \sqrt{E_{\max}/\eta} \\ E_{\max}, & \text{for } r_0 + \sqrt{E_{\max}/\eta} \leq \|\mathbf{r} - \mathbf{R}_k\| \end{cases} \quad (3.10)$$

The total CAP for the N_A atoms takes the form

$$v_{\text{CAP}}(\mathbf{r}) = \min \{ f_1^{\text{CAP}}(\mathbf{r}), \dots, f_{N_A}^{\text{CAP}}(\mathbf{r}) \} \quad (3.11)$$

The cut-off radius r_0 should be small enough to affect the electron density (because of the finite extent of the basis). In the mean while, large enough to not overly perturb the original system. The optimal parameters may be system-, theory-, basis-dependent, etc. In this work, we use a compromise value $r_0 = 9.524 \text{ a.u.} \approx 5.040 \text{ \AA}$ for all calculations and focus on the improvement of broken symmetry between spin-restricted and spin-unrestricted formulations. The curvature is chosen to be the typical value $\eta = 4.0 \text{ a.u.}$ [71]. The CAP is cut off at the maximum $E_{\max} = 10 \text{ hartree}$ to avoid numerical overflow. [71]

The total external potential $v(\mathbf{r}, t)$ is then

$$v(\mathbf{r}, t) = v_{\text{ne}}(\mathbf{r}) + v_{\text{laser}}(\mathbf{r}, t) - iv_{\text{CAP}}(\mathbf{r}) \quad (3.12)$$



where $v_{\text{ne}}(\mathbf{r})$ is the external potential of the nucleus.

For the time propagation, the small enough time step $\Delta t = 0.02 \text{ a.u.} (\approx 0.484 \text{ as})$ is chosen.[58] The total propagation length is chosen to be the same as the length of the laser pulse, $t_1 - t_0 = 1000 \text{ a.u.} \approx 24.1 \text{ fs.}$ [66] The modified-midpoint unitary transform (MMUT) is adopted to construct the propagator.[58, 72]

The equilibrium geometry of H_2 is chosen to be 1.45 a.u. $\approx 0.767 \text{ \AA}$, which is around that optimized with the spin-restricted KS-LDA. The stretched geometry of H_2 is chosen to be 3.78 a.u. ($\approx 2.00 \text{ \AA}$), where the multi-reference character is unneglectable.[2] Following are the results of H_2 positioned along the z -axis (parallel to the laser polarization) with the center of mass being the origin. The results of the systems perpendicular to the laser polarization duplicate and are complemented in appendix A.

3.4 H_2 at the Equilibrium Geometry

The complete discussions and the optimization of the HHG spectra are not the aim of this work. Instead, numerous successful applications of TDKS to HHG[8] serve as a reference to assess RT-TAO. While in the mean time, the limitations of KS-DFT and TDKS in multi-reference systems provide a suitable stage for RT-TAO to improve upon.

H_2 at the equilibrium geometry is a single-reference system, thus we expect TDKS-ALDA to grasp the characteristics of the HHG spectra. Figure 3.2 shows the HHG spectra

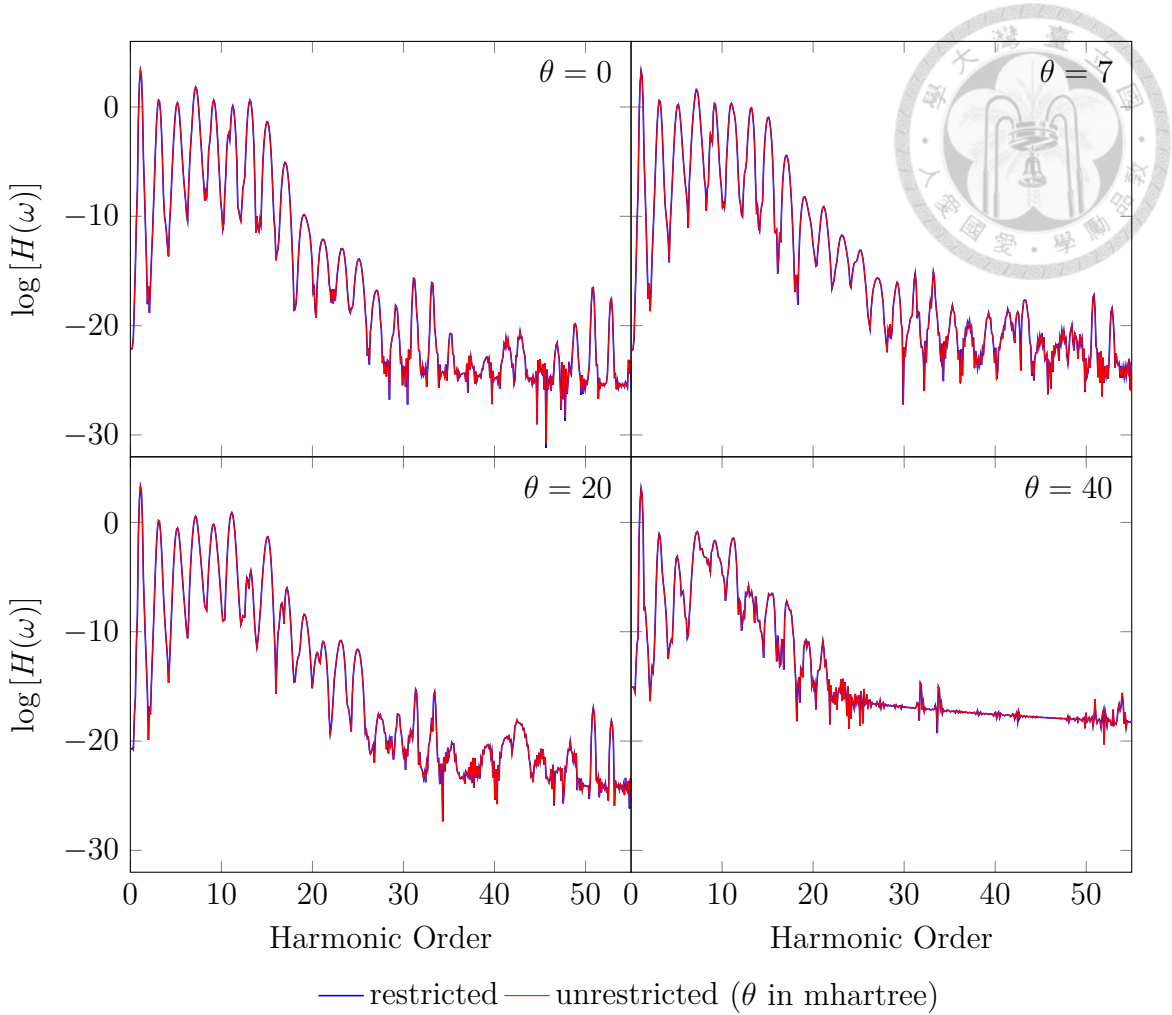


Figure 3.2: HHG spectra of H_2 at 1.45 a.u.. $\theta = 0$ corresponds to TDKS-ALDA.

for different θ . For $\theta = 0$ (TDKS-ALDA), we see TDKS-ALDA indeed does so. The HHG spectrum starts with the highest intensity of the first harmonic, followed by a rapid decrease in intensity of the third harmonic, the plateau with constant intensities up to the 15th harmonic, and an abrupt cut-off over the 17th harmonic. Only odd harmonics are present because of the inversion symmetry of the system.[8] As for the non-monotonic intensities over the 31th harmonic, they may not be a problem due to the logarithmically low relative intensities. They may be attributed to the finite extent of Gaussian basis,[5] the unutilized ghost atom functions,[66] or the over-largeness of the cut-off radius r_0 , or others. As formerly stated, they are not the aim of this work, and we would stop here.

Spin-restricted and spin-unrestricted TDKS-ALDA produce similar results, as they

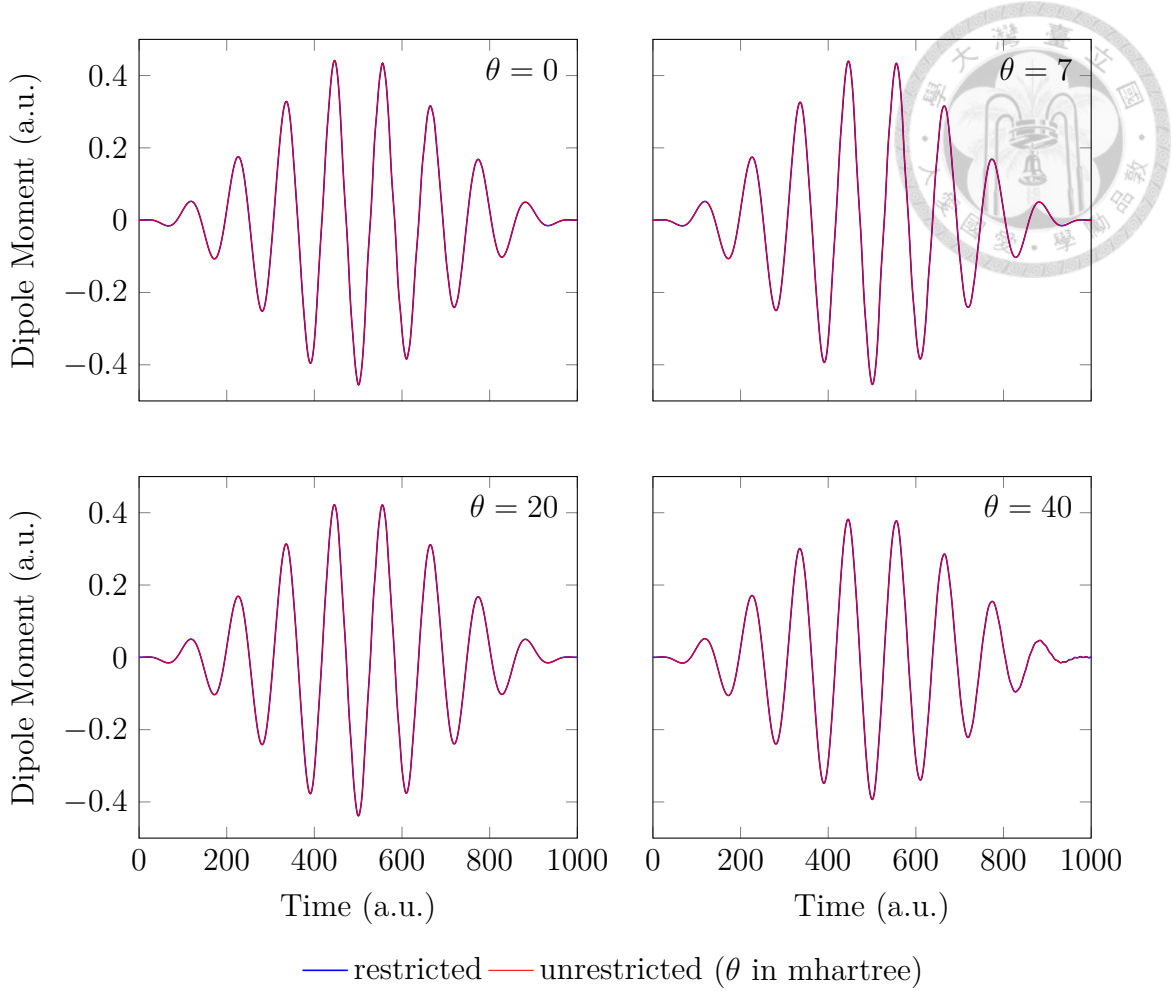


Figure 3.3: Induced dipole moment of H_2 at 1.45 a.u.. $\theta = 0$ corresponds to TDKS-ALDA.

should do at the limit of exact TDKS. For $\theta = 7$ mhartree, the HHG spectra are similar to TDKS-ALDA, and we would not repeat here. For $\theta = 20$ mhartree, the HHG spectra show a slight deviation of the 13th harmonic. For $\theta = 40$ mhartree, even the range of plateau differs.

For completeness, some other time-dependent observables are shown. Figure 3.3 shows the induced dipole moment and fig. 3.4 shows the number of bound electrons. For $\theta = 40$ mhartree, the number of bound electrons is even qualitatively different from the others, hinting at the inappropriateness of over-large θ in a single-reference system. Ideally, θ should be chosen such that the occupation numbers (TOONs) resemble the natural orbital occupation numbers (NOONs).[2]

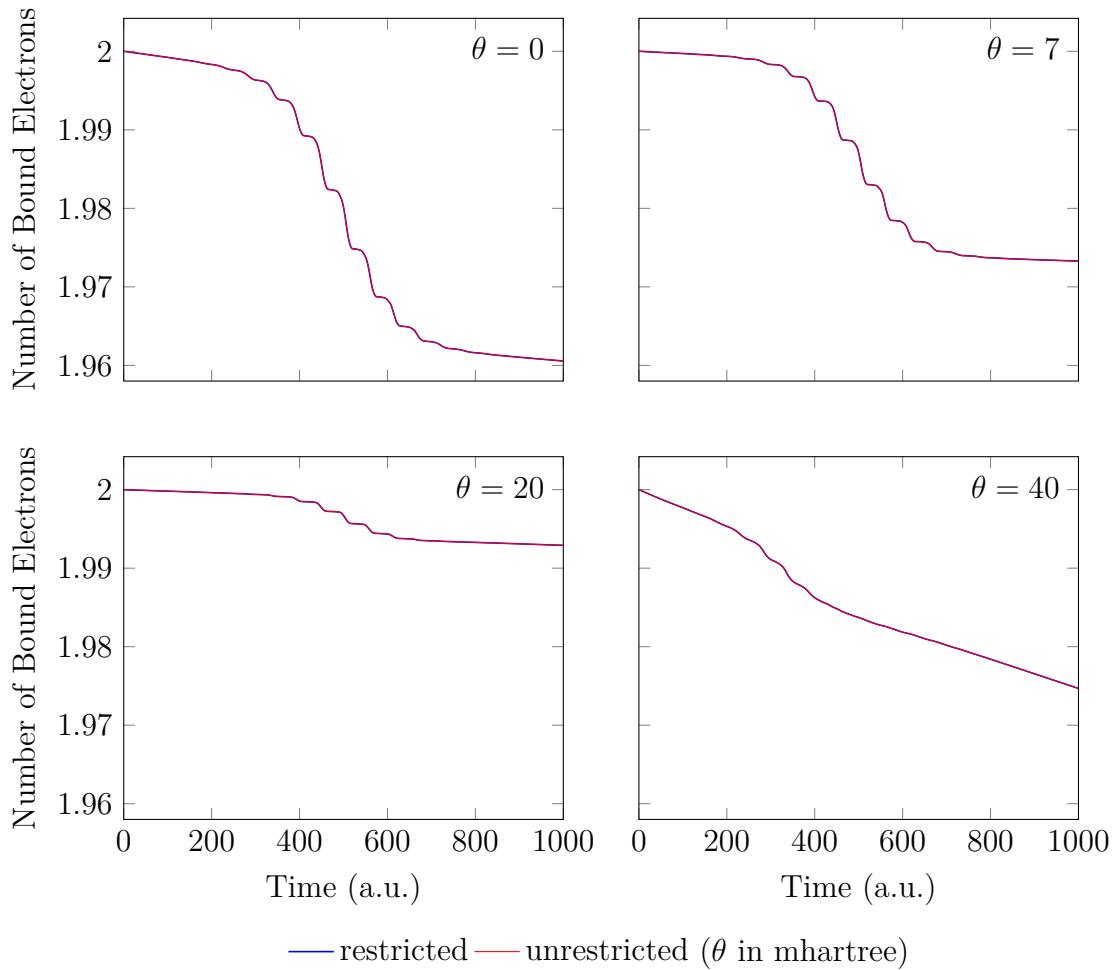


Figure 3.4: Number of bound electrons of H_2 at 1.45 a.u.. $\theta = 0$ corresponds to TDKS-ALDA.

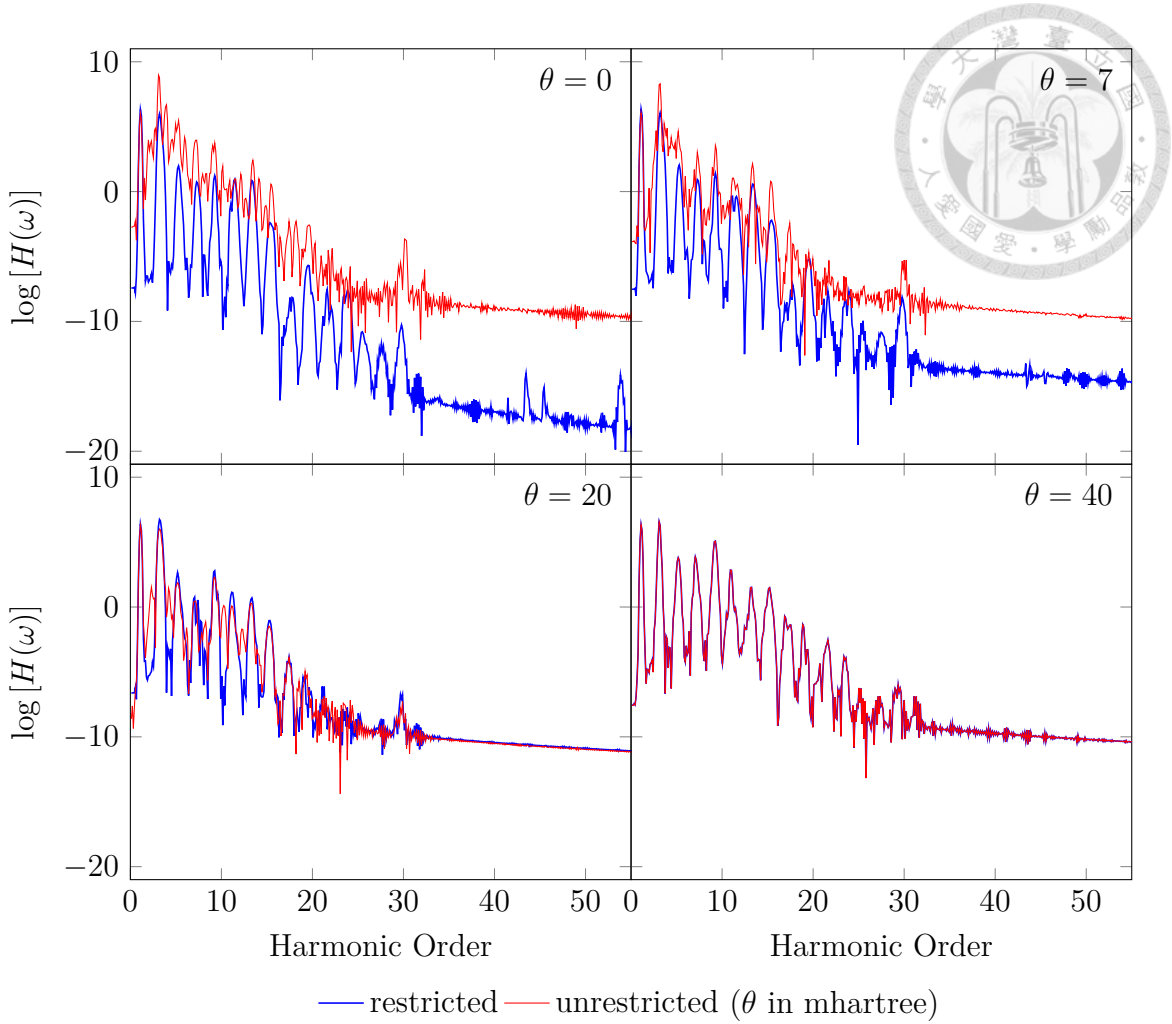


Figure 3.5: HHG spectra of H_2 at 3.78 a.u.. $\theta = 0$ corresponds to TDKS-ALDA.

3.5 H_2 at the Stretched Geometry

Next, we examine H_2 at the stretched geometry, which is the simplest two-electron system with unneglectable multi-reference characters. Figure 3.5 shows the HHG spectra for different θ . For $\theta = 0$ (TDKS-ALDA), the spin-restricted HHG spectrum starts with the highest intensities of the first and the third harmonics, followed by a rapid decrease in intensity of the 5th harmonic, the plateau with constant intensities up to the 13th harmonic, and an abrupt cut-off over the 15th harmonic. Other similar characteristics are as at the equilibrium geometry, and we would not repeat here.

However, unrestricted TDKS-ALDA produces significantly different results from restricted TDKS-ALDA and seems overwhelmed by the noise. We refer to this as the broken symmetry of spin-restricted and spin-unrestricted formulations. As θ increases, the spin-restricted spectra slightly deviate, with the spin-unrestricted spectra becoming more similar to the spin-restricted ones. For $\theta = 40$ mhartree, restricted and unrestricted RT-TAO-ALDA produce similar results, as they should do at the limit of exact RT-TAO.

For completeness, some other time-dependent observables are shown. Figure 3.6 shows the induced dipole moment, and fig. 3.7 shows the number of bound electrons. For these time-dependent observables, improvements of the broken symmetry enhance as θ increases. For $\theta = 40$ mhartree, restricted and unrestricted RT-TAO-ALDA produce similar results.

3.6 Discussions of Symmetry-Breaking Effects

When it comes to spin-symmetric systems, both the exact spin-restricted and spin-unrestricted formulations should produce the same results. However, the unknown and necessarily approximated functionals (density functional approximation, i.e., DFA), including the XC functional and the θ functional, etc, may cause unphysical symmetry-breaking effects.[\[73\]](#)

For single-reference systems (e.g., H_2 at the equilibrium geometry), the restricted and unrestricted formulations do produce similar ground-state energies for KS-LDA and TAO-LDA, respectively,[\[2\]](#) and do produce similar HHG spectra for TDKS-ALDA and RT-TAO-ALDA, respectively. But this is not the case for multi-reference systems (e.g., H_2 at the stretched geometry). While TAO-LDA and RT-TAO-ALDA remain producing

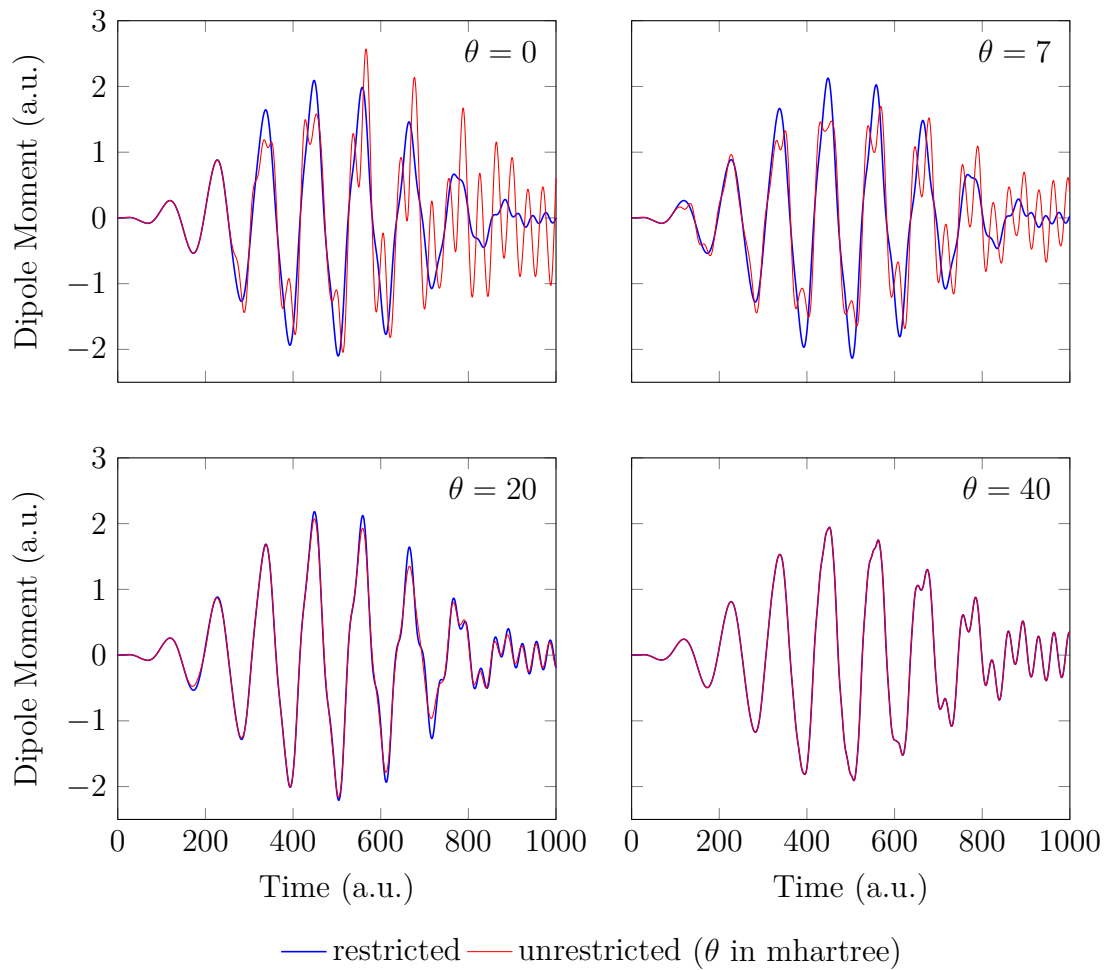


Figure 3.6: Induced dipole moment of H_2 at 3.78 a.u.. $\theta = 0$ corresponds to TDKS-ALDA.

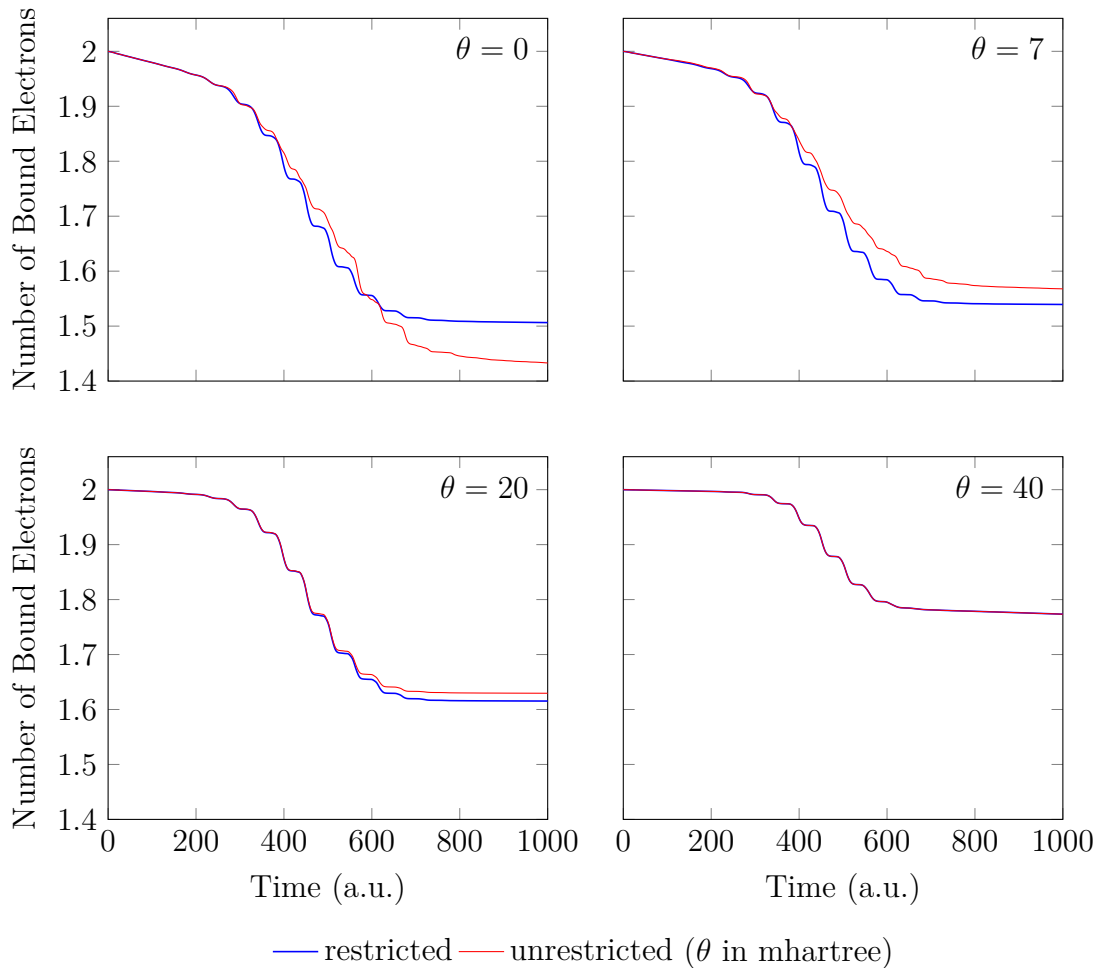
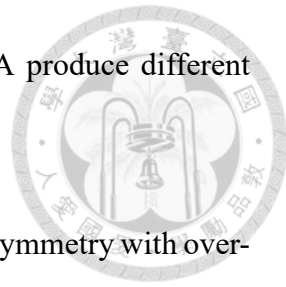


Figure 3.7: Number of bound electrons of H_2 at 3.78 a.u.. $\theta = 0$ corresponds to TDKS-ALDA.

similar results with sufficiently large θ , KS-LDA and TDKS-ALDA produce different ones.[2]

Specifically, spin-restricted KS-LDA preserves the correct spin-symmetry with over-estimations of the ground-state energies,[2] while unrestricted KS-LDA predicts lower ground-state energies than restricted KS-LDA at the cost of unphysically breaking the spin-symmetry.[2] On the other hand, as shown in section 3.5, unrestricted TDKS-ALDA produces rather noisy HHG spectra and restricted TDKS-ALDA may be the only viable option of TDKS-ALDA.

Furthermore, by observing the spin-unrestricted formulation of RT-TAO, we know if $f_i^\alpha = f_i^\beta$, $\phi_i^\alpha(\mathbf{r}, t_0) = \phi_i^\beta(\mathbf{r}, t_0)$, and $n^\alpha(\mathbf{r}, t_0) = n^\beta(\mathbf{r}, t_0)$, then unrestricted RT-TAO-ALDA is spin-symmetric and produces same results as restricted RT-TAO-ALDA. Since TAO schemes with $\theta = 0$ reduce to KS schemes, the only possible reason for the failure of unrestricted TDKS-ALDA (in the sense of the broken symmetry of restricted and unrestricted formulations) is the broken symmetry of spin-up and spin-down electrons of unrestricted KS-LDA (f_i^σ , $\phi_i^\sigma(\mathbf{r}, t_0)$, or $n^\sigma(\mathbf{r}, t_0)$). This highlights the importance of TAO-LDA. To confirm or to double-check the above arguments, we have run restricted TAO-LDA followed by unrestricted RT-TAO-ALDA. Unrestricted RT-TAO-ALDA in such case does produce similar results as restricted RT-TAO-ALDA.





Chapter 4 Conclusions

In this work, we propose RT-TAO, a real-time time-dependent extension of TAO-DFT, or the TAO version of RT-TD-DFT. We revise the ill-defined $\text{HXC}\theta$ action functional in TDTAO and apply RT-TAO-ALDA to HHG. The results show that RT-TAO-ALDA preserves the abilities of TAO-LDA to handle multi-reference systems and outperforms RT-TD-ALDA in multi-reference systems in the view of spin-symmetry of restricted and unrestricted formulations.

In chapter 1, we begin with the difficulties in solving the Schrödinger equation even with the BO approximation. Numerical methods are a must, with wave function-based methods limited by their demanding computational cost, and DFT the balanced option. Fundamental theorems such as the HK theorems and Mermin's theorems, along with the KS scheme and the TAO scheme, are introduced. The NI-PS v_s -representability of the ground state density is emphasized because it is the key difference between KS-DFT and TAO-DFT, which makes TAO-LDA outperform KS-LDA in multi-reference systems.

Following the ground-state theories are the time-dependent theories, aiming to solve the time-dependent Schrödinger equation. The RG theorems, the van Leeuwen theorem, and their ensemble extensions are introduced. We mention the applications and limitations of LR-TD-DFT, RT-TD-DFT, and TDTAO. These form the background of the proposal of

RT-TAO.

For completeness, in section 2.1, we first give a summary of the iterative procedure of ground-state TAO-DFT, including both spin-restricted and spin-unrestricted formulations.

The ill-defined HXC θ action functional in TDTAO is highlighted in section 2.2. In section 2.3, we start with the ensemble extensions of the RG theorems and the van Leeuwen theorem and propose the RT-TAO scheme. The expression of the TAO ensemble matching the definition in section 2.3 is given in section 2.4. Because the electron number can vary in the TAO ensemble, which one may not be familiar with, we give a demonstration of combining one-electron states to form a basis of Fock space in section 2.5. The relation of the ensemble average and one-electron states is derived in section 2.6. In section 2.7, we give the expression of the RT-TAO potential, which is intimate with $A_{XC\theta}[n]$. The adiabatic approximations for the HXC θ potential are explicitly given in section 2.9. Finally, a summary of the practical scheme of RT-TAO, including spin-restricted and spin-unrestricted formulations, is given in section 2.10.

To assess RT-TAO, we apply it to H₂ to simulate HHG. A brief introduction of HHG is given in section 3.1. Time-dependent observables are defined in sections 3.1 and 3.2. Computational details are provided in section 3.3. In section 3.4, for H₂ at the equilibrium geometry, which is a single-reference system, TDKS-ALDA and RT-TAO-ALDA perform well and preserve spin-symmetry. In section 3.5, for H₂ at the stretched geometry, which is a multi-reference system, spin-unrestricted TDKS-ALDA fails to produce similar results as spin-restricted TDKS-ALDA. On the other hand, spin-unrestricted RT-TAO-ALDA, improves upon this issue with increasing θ , and produces similar results as spin-restricted RT-TAO-ALDA with sufficiently large θ . Symmetry-breaking effects are discussed in section 3.6, with the broken symmetry of restricted and unrestricted TDKS-ALDA attributed



to the broken symmetry of spin-up and spin-down electrons of unrestricted KS-LDA.

As the final note, while the determination of θ remains an open question (θ should be chosen such that the TOONs resemble the NOONs[2]), for single-reference systems, θ should be relatively small, and RT-TAO-ALDA performs similar to TDKS-ALDA. For multi-reference systems, θ should be relatively large, and unrestricted RT-TAO-ALDA outperforms unrestricted TDKS-ALDA in the view of preserving the spin-symmetry of restricted and unrestricted formulations.





References

- [1] W. Kohn and L. J. Sham, Phys. Rev. **140**, A1133 (1965).
- [2] J.-D. Chai, The Journal of Chemical Physics **136**, 154104 (2012).
- [3] J.-D. Chai, The Journal of Chemical Physics **140**, 18A521 (2014).
- [4] J.-D. Chai, The Journal of Chemical Physics **146**, 044102 (2017).
- [5] Y. Zhu and J. M. Herbert, The Journal of Chemical Physics **156**, 204123 (2022).
- [6] S.-H. Yeh, A. Manjanath, Y.-C. Cheng, J.-D. Chai, and C.-P. Hsu, The Journal of Chemical Physics **153**, 084120 (2020).
- [7] M. Born and R. Oppenheimer, Annalen der Physik **389**, 457 (1927).
- [8] C. Ullrich, Time-Dependent Density-Functional Theory: Concepts and Applications, Oxford Graduate Texts (OUP Oxford, 2012), ISBN 9780199563029.
- [9] P. Hohenberg and W. Kohn, Phys. Rev. **136**, B864 (1964).
- [10] E. Engel and R. M. Dreizler, Foundations of Density Functional Theory: Existence Theorems (Springer Berlin Heidelberg, Berlin, Heidelberg, 2011), pp. 11–56, ISBN 978-3-642-14090-7.
- [11] T. L. Gilbert, Phys. Rev. B **12**, 2111 (1975).

[12] M. Levy, *Proceedings of the National Academy of Sciences* **76**, 6062 (1979).

[13] E. H. Lieb, *International Journal of Quantum Chemistry* **24**, 243 (1983).

[14] R. M. Dreizler and E. K. U. Gross, *Density Functional Theory: An Approach to the Quantum ManyBody Problem* (Springer Berlin Heidelberg, Berlin, Heidelberg, 1990), ISBN 978-3-642-86105-5.

[15] M. Levy, *Phys. Rev. A* **26**, 1200 (1982).

[16] P. Schipper, O. Gritsenko, and E. Baerends, *Theoretical Chemistry Accounts* **99**, 329 (1998), ISSN 1432-881X.

[17] R. C. Morrison, *The Journal of Chemical Physics* **117**, 10506 (2002).

[18] J. Katriel, S. Roy, and M. Springborg, *The Journal of Chemical Physics* **121**, 12179 (2004).

[19] A. D. Becke, *The Journal of Chemical Physics* **138**, 074109 (2013).

[20] N. D. Mermin, *Phys. Rev.* **137**, A1441 (1965).

[21] V. V. Flambaum, F. M. Izrailev, and G. Casati, *Phys. Rev. E* **54**, 2136 (1996).

[22] V. V. Flambaum and F. M. Izrailev, *Phys. Rev. E* **55**, R13 (1997).

[23] V. V. Flambaum and F. M. Izrailev, *Phys. Rev. E* **56**, 5144 (1997).

[24] F. Xuan, J.-D. Chai, and H. Su, *ACS Omega* **4**, 7675 (2019), pMID: 31459859.

[25] C.-Y. Lin, K. Hui, J.-H. Chung, and J.-D. Chai, *RSC Adv.* **7**, 50496 (2017).

[26] B.-J. Chen and J.-D. Chai, *RSC Adv.* **12**, 12193 (2022).

[27] S. Li and J.-D. Chai, *Frontiers in Chemistry* **8** (2020), ISSN 2296-2646.

[28] C.-S. Wu and J.-D. Chai, *Journal of Chemical Theory and Computation* **11**, 2003 (2015).



[29] C.-N. Yeh and J.-D. Chai, *Scientific Reports* **6**, 30562 (2016).

[30] S. Seenithurai and J.-D. Chai, *Scientific Reports* **6** (2016).

[31] C.-S. Wu, P.-Y. Lee, and J.-D. Chai, *Scientific Reports* **6**, 37249 (2016).

[32] S. Seenithurai and J.-D. Chai, *Scientific Reports* **7**, 4966 (2017).

[33] S. Seenithurai and J.-D. Chai, *Scientific Reports* **8** (2018).

[34] C.-N. Yeh, C. Wu, H. Su, and J.-D. Chai, *RSC Adv.* **8**, 34350 (2018).

[35] J.-H. Chung and J.-D. Chai, *Scientific Reports* **9**, 2907 (2019).

[36] S. Seenithurai and J.-D. Chai, *Scientific Reports* **9**, 12139 (2019).

[37] Q. Deng and J.-D. Chai, *ACS Omega* **4**, 14202 (2019), pMID: 31508542.

[38] H.-J. Huang, S. Seenithurai, and J.-D. Chai, *Nanomaterials* **10** (2020), ISSN 2079-4991.

[39] S. Seenithurai and J.-D. Chai, *Scientific Reports* **10**, 13133 (2020).

[40] S. Seenithurai and J.-D. Chai, *Nanomaterials* **11** (2021), ISSN 2079-4991.

[41] C.-C. Chen and J.-D. Chai, *Nanomaterials* **12** (2022), ISSN 2079-4991.

[42] E. Runge and E. K. U. Gross, *Phys. Rev. Lett.* **52**, 997 (1984).

[43] R. van Leeuwen, *Phys. Rev. Lett.* **82**, 3863 (1999).

[44] T.-c. Li and P.-q. Tong, *Phys. Rev. A* **31**, 1950 (1985).

[45] T. Li and Y. Li, Phys. Rev. A **31**, 3970 (1985).

[46] A. Pribram-Jones, P. E. Grabowski, and K. Burke, Phys. Rev. Lett. **116**, 233001 (2016).

[47] J. Dufty, K. Luo, and S. B. Trickey, Phys. Rev. E **98**, 033203 (2018).

[48] J. P. Solovej (2014), <https://web.math.ku.dk/solovej/MANYBODY/mbnotes-ptn-5-3-14.pdf>.

[49] R. Seiringer, Cold Quantum Gases and Bose–Einstein Condensation (Springer Berlin Heidelberg, Berlin, Heidelberg, 2012), pp. 55–92, ISBN 978-3-642-29511-9.

[50] M. Greiner, P. Carrier, and A. Görling, Phys. Rev. B **81**, 155119 (2010).

[51] R. Shankar, Principles of Quantum Mechanics, 经典英文学教材系列 (Springer, 1994), ISBN 9780306447907.

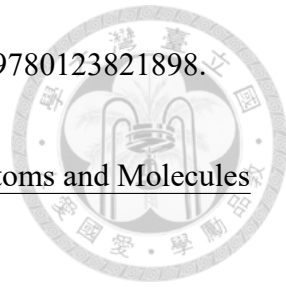
[52] C. Heunen and J. Vicary, Categories for Quantum Theory: An Introduction, Oxford Graduate Texts in Mathematics (OUP Oxford, 2019), ISBN 9780191060069.

[53] N. Dunford and J. Schwartz, Linear Operators: General theory, Linear Operators (Interscience Publishers, 1958), ISBN 9780470226056.

[54] R. Martin, Electronic Structure: Basic Theory and Practical Methods (Cambridge University Press, 2020), ISBN 9781108429900.

[55] gigo318 (<https://physics.stackexchange.com/users/297482/gigo318>), Operator expectation value for system of non-interacting particles (fermions), Physics Stack Exchange, uRL:<https://physics.stackexchange.com/q/653616> (version: 2021-07-27).





[56] P. Beale, Statistical Mechanics (Elsevier Science, 2011), ISBN 9780123821898.

[57] R. G. Parr and Y. Weitao, in Density-Functional Theory of Atoms and Molecules (Oxford University Press, 1995), ISBN 9780195092769.

[58] Y. Zhu and J. M. Herbert, *The Journal of Chemical Physics* **148**, 044117 (2018).

[59] M. Lewenstein, P. Balcou, M. Y. Ivanov, A. L'Huillier, and P. B. Corkum, *Phys. Rev. A* **49**, 2117 (1994).

[60] P. B. Corkum, *Phys. Rev. Lett.* **71**, 1994 (1993).

[61] F. Bedurke, T. Klamroth, P. Krause, and P. Saalfrank, *The Journal of Chemical Physics* **150**, 234114 (2019).

[62] E. Epifanovsky, A. T. B. Gilbert, X. Feng, J. Lee, Y. Mao, N. Mardirossian, P. Pokhilko, A. F. White, M. P. Coons, A. L. Dempwolff, et al., *The Journal of Chemical Physics* **155**, 084801 (2021).

[63] B. P. Pritchard, D. Altarawy, B. Didier, T. D. Gibson, and T. L. Windus, *Journal of Chemical Information and Modeling* **59**, 4814 (2019), pMID: 31600445.

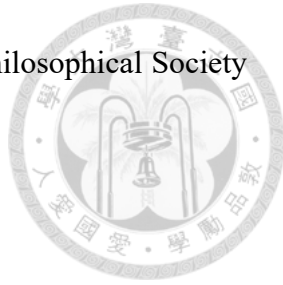
[64] T. H. Dunning, *The Journal of Chemical Physics* **90**, 1007 (1989).

[65] R. A. Kendall, T. H. Dunning, and R. J. Harrison, *The Journal of Chemical Physics* **96**, 6796 (1992).

[66] F. Bedurke, T. Klamroth, and P. Saalfrank, *Phys. Chem. Chem. Phys.* **23**, 13544 (2021).

[67] C. W. Murray, N. C. Handy, and G. J. Laming, *Molecular Physics* **78**, 997 (1993).

[68] P. A. M. Dirac, Mathematical Proceedings of the Cambridge Philosophical Society **26**, 376–385 (1930).



[69] J. P. Perdew and Y. Wang, Phys. Rev. B **45**, 13244 (1992).

[70] J. Maurer and U. Keller, Journal of Physics B: Atomic, Molecular and Optical Physics **54**, 094001 (2021).

[71] Y. Zhu, B. Alam, and J. Herbert, ChemRxiv (2021).

[72] X. Li, S. M. Smith, A. N. Markevitch, D. A. Romanov, R. J. Levis, and H. B. Schlegel, Phys. Chem. Chem. Phys. **7**, 233 (2005).

[73] A. J. Cohen, P. Mori-Sánchez, and W. Yang, Science **321**, 792 (2008).



Appendix A — Systems Perpendicular to the Laser Polarization

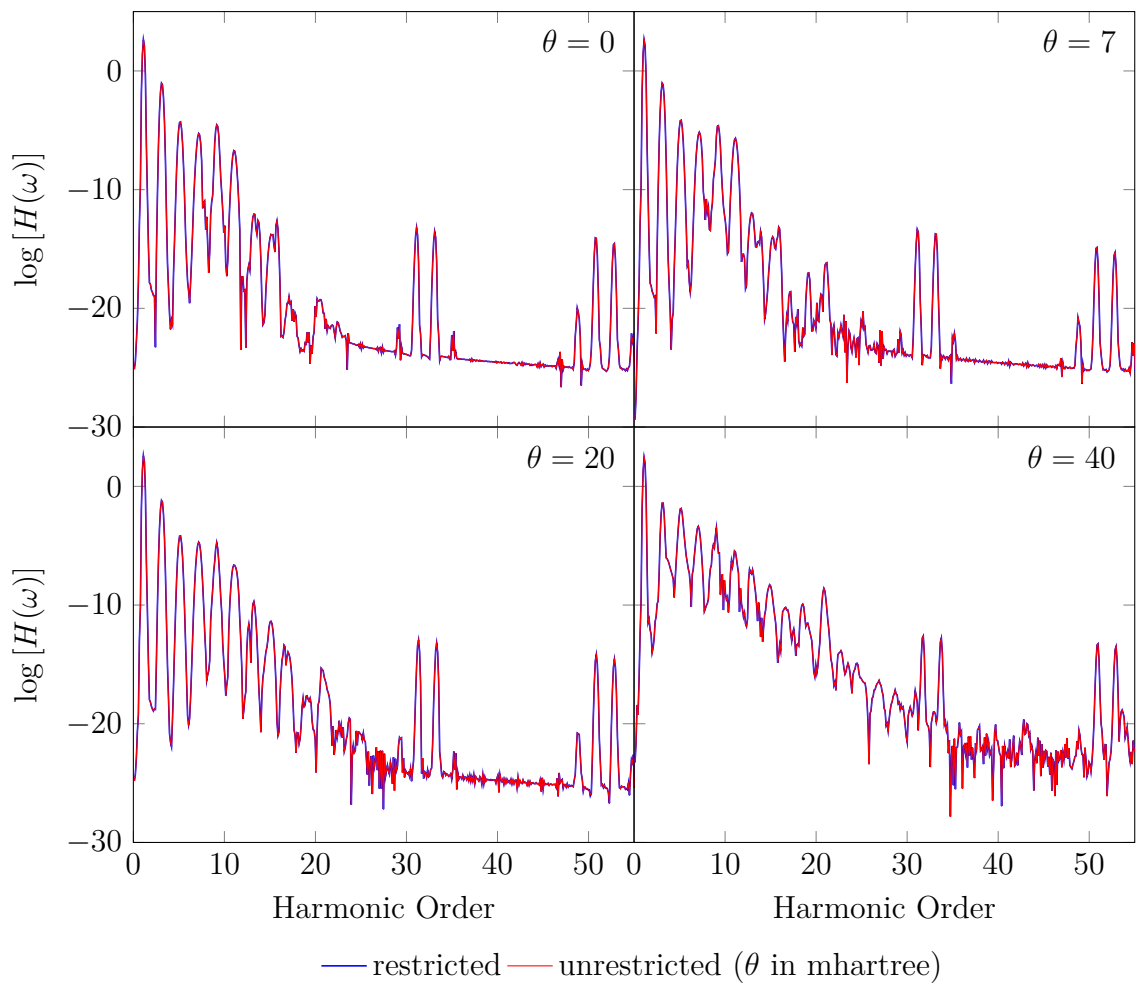


Figure A.1: HHG spectra of H_2 at 1.45 a.u. aligned perpendicular to the laser polarization. $\theta = 0$ corresponds to TDKS-ALDA.

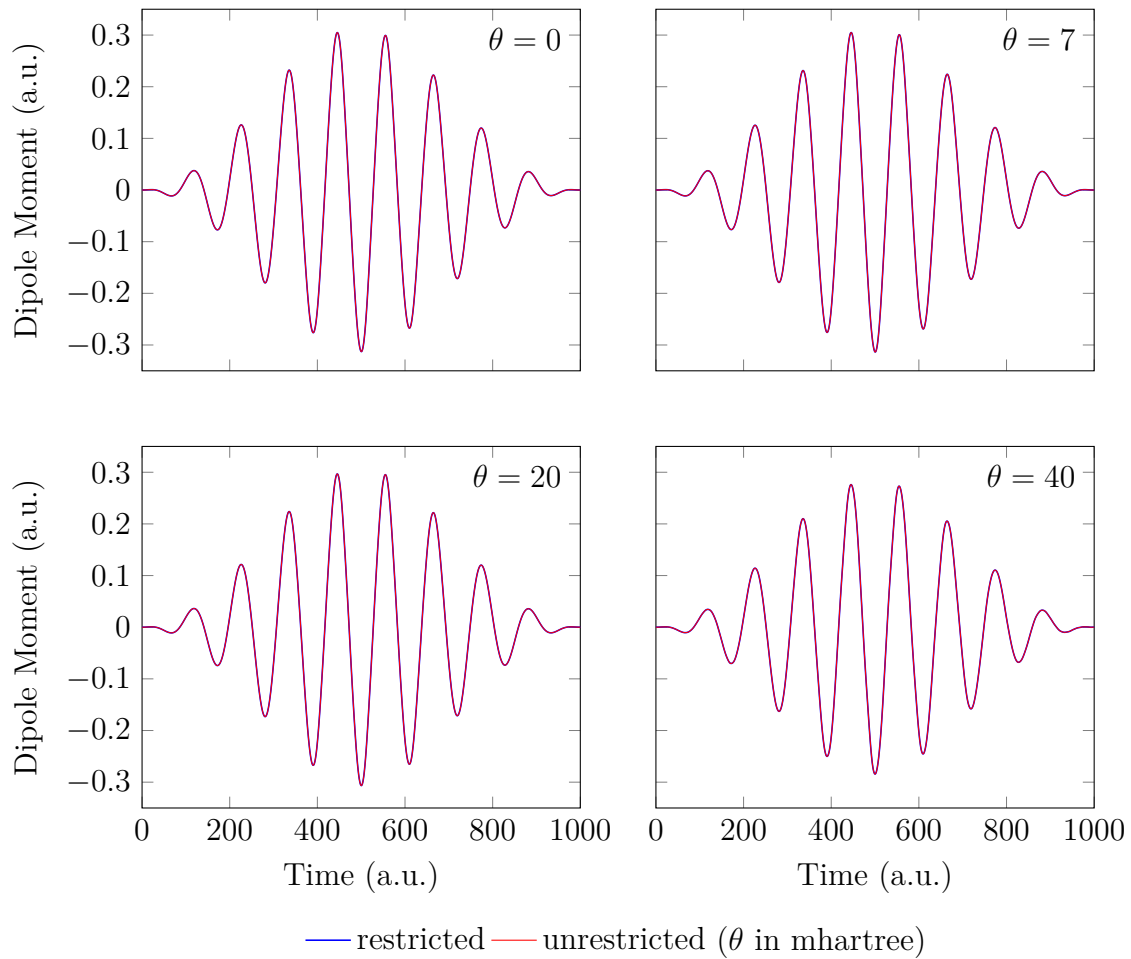


Figure A.2: Induced dipole moment of H_2 at 1.45 a.u. aligned perpendicular to the laser polarization. $\theta = 0$ corresponds to TDKS-ALDA.

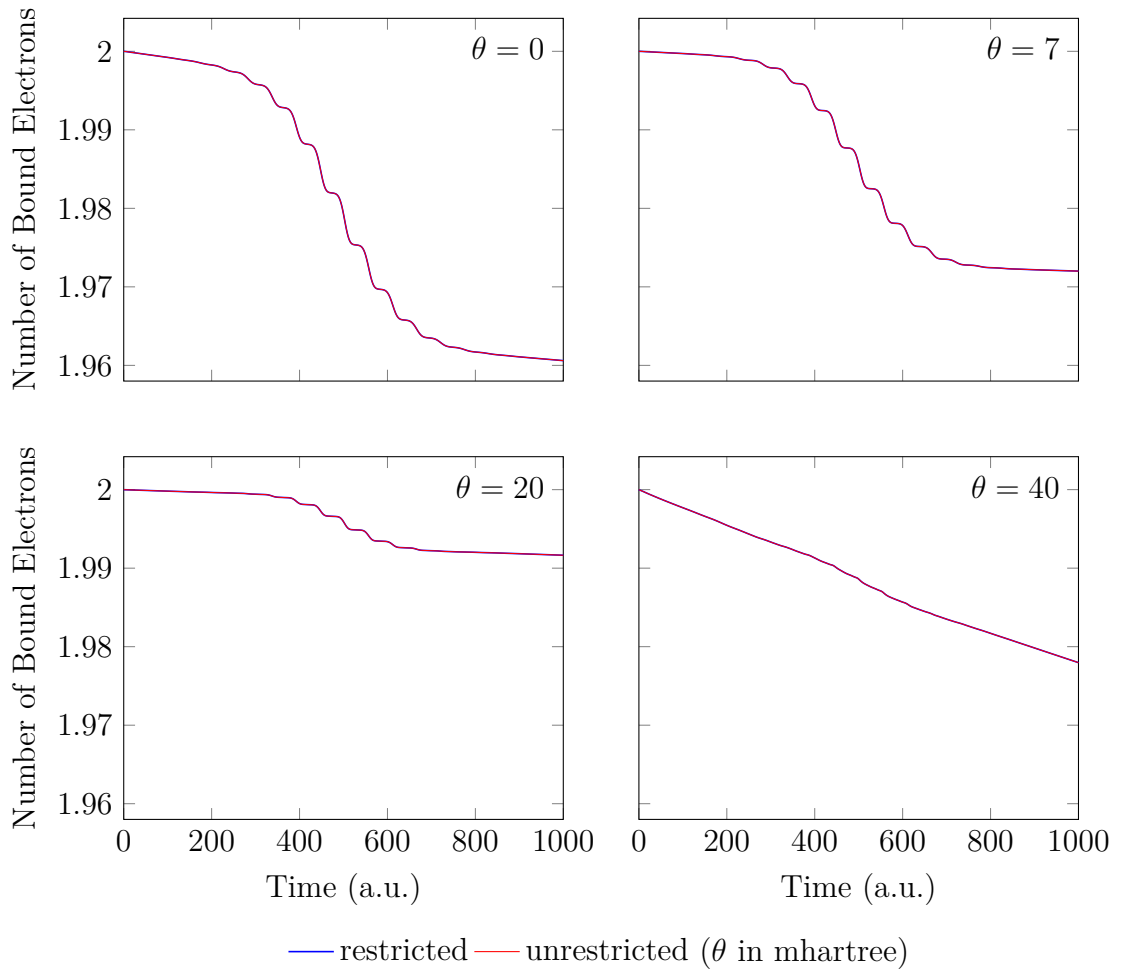


Figure A.3: Number of bound electrons of H_2 at 1.45 a.u. aligned perpendicular to the laser polarization. $\theta = 0$ corresponds to TDKS-ALDA.

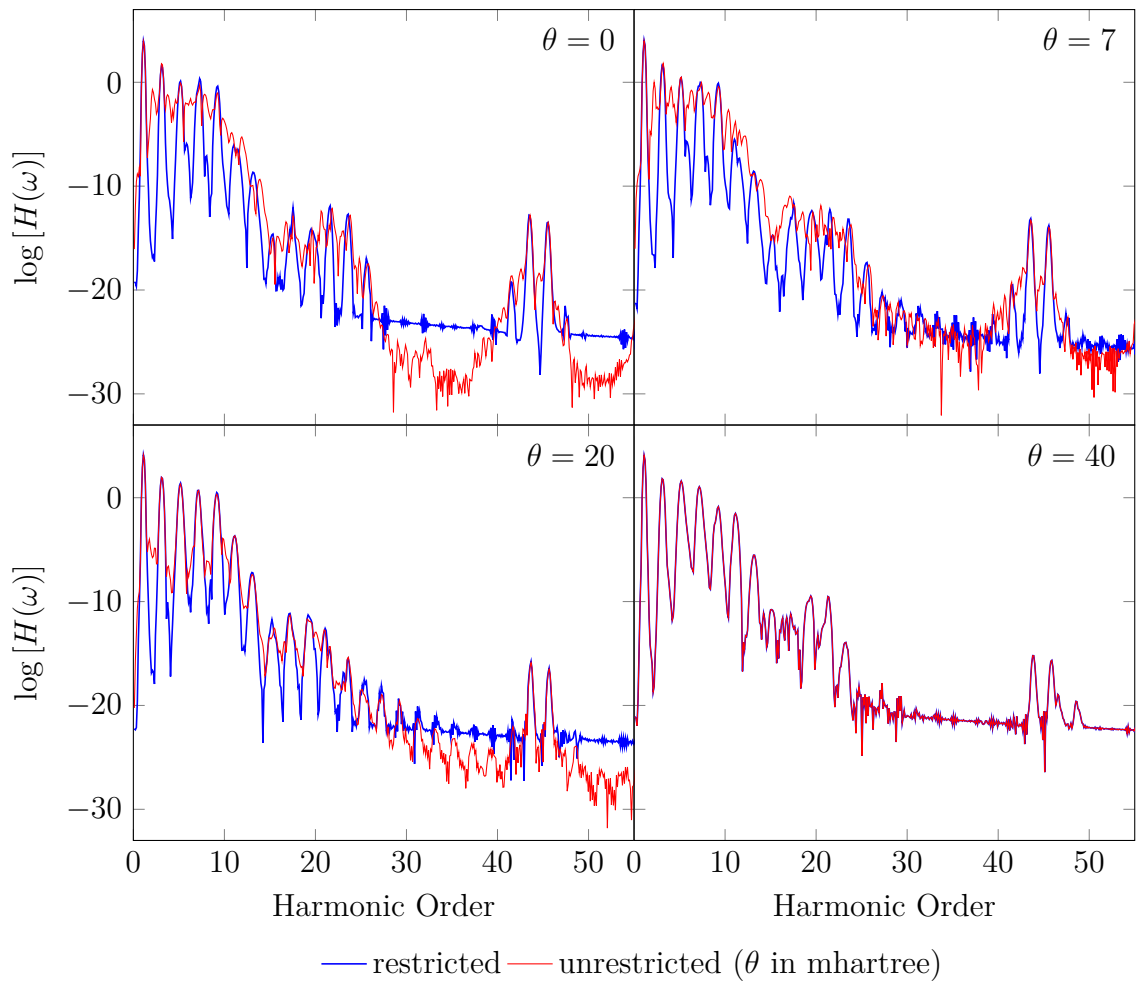


Figure A.4: HHG spectra of H_2 at 3.78 a.u. aligned perpendicular to the laser polarization. $\theta = 0$ corresponds to TDKS-ALDA.

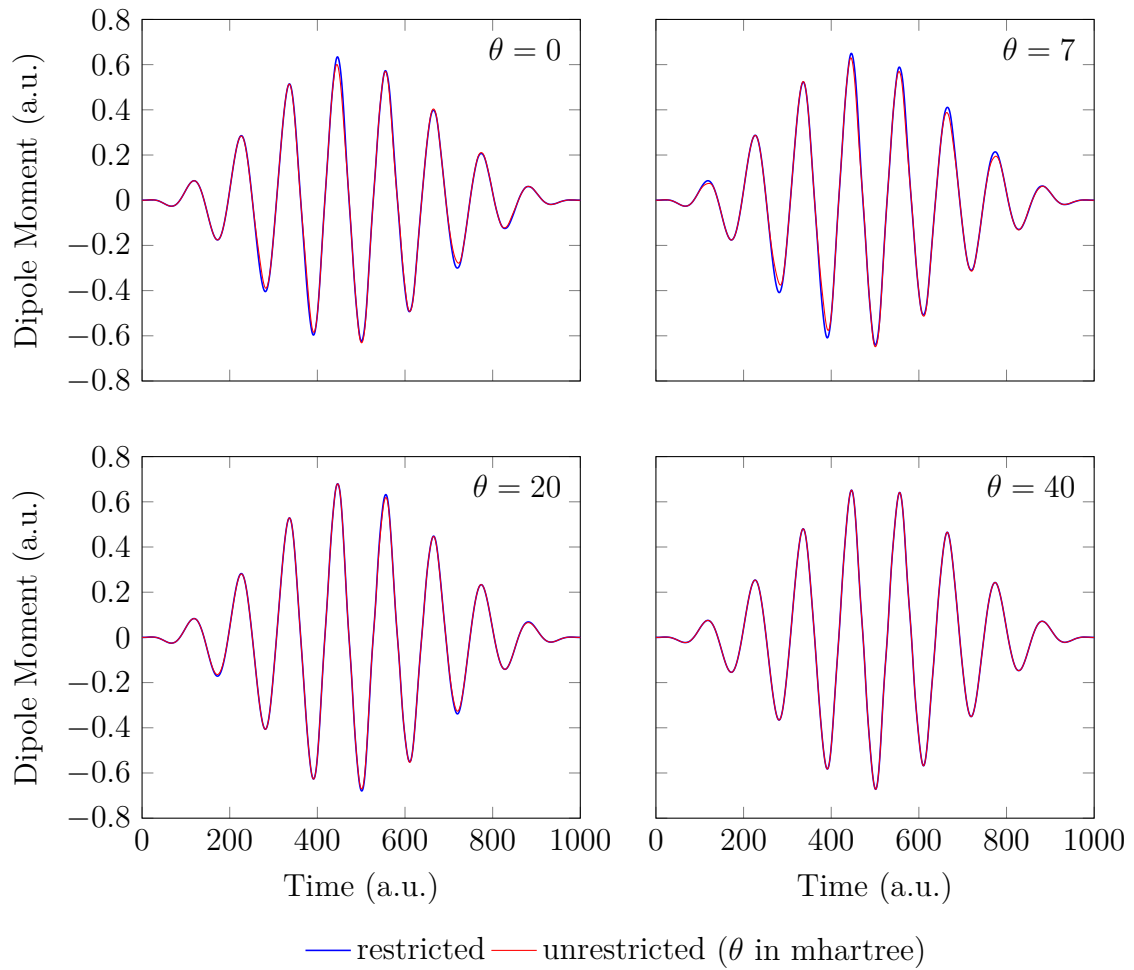


Figure A.5: Induced dipole moment of H_2 at 3.78 a.u. aligned perpendicular to the laser polarization. $\theta = 0$ corresponds to TDKS-ALDA.

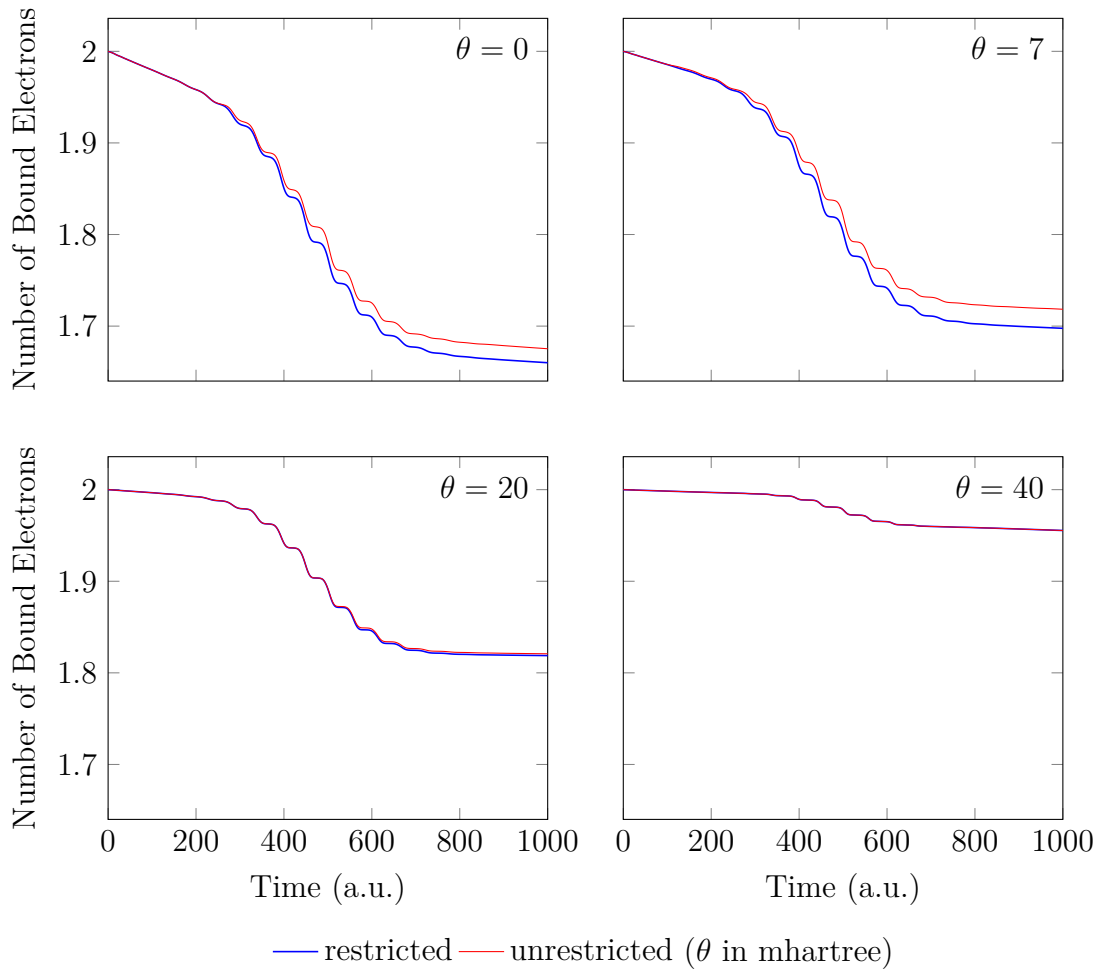


Figure A.6: Number of bound electrons of H_2 at 3.78 a.u. aligned perpendicular to the laser polarization. $\theta = 0$ corresponds to TDKS-ALDA.





Appendix B — HHG Spectra without Window Functions

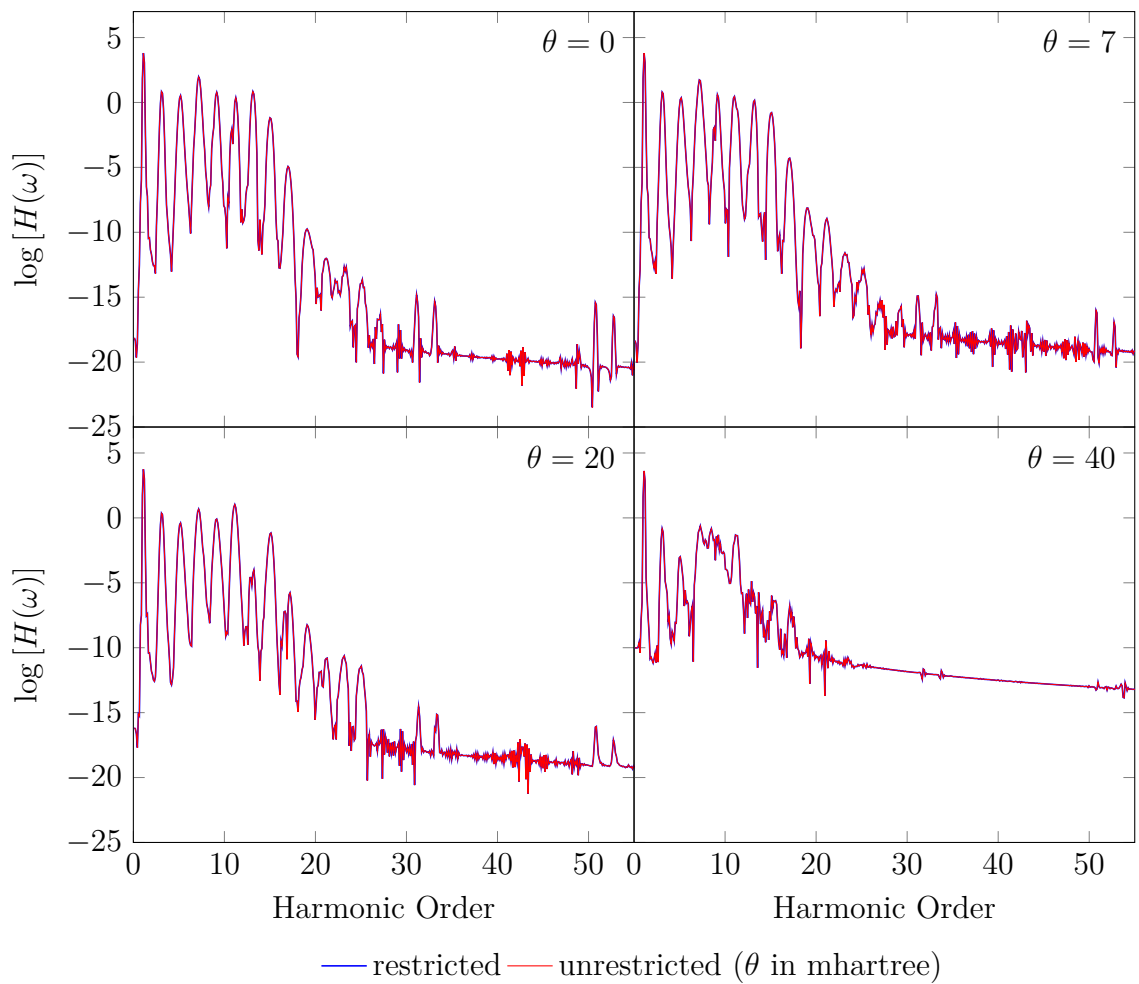


Figure B.7: HHG spectra of H_2 at 1.45 a.u. without window function. $\theta = 0$ corresponds to TDKS-ALDA.

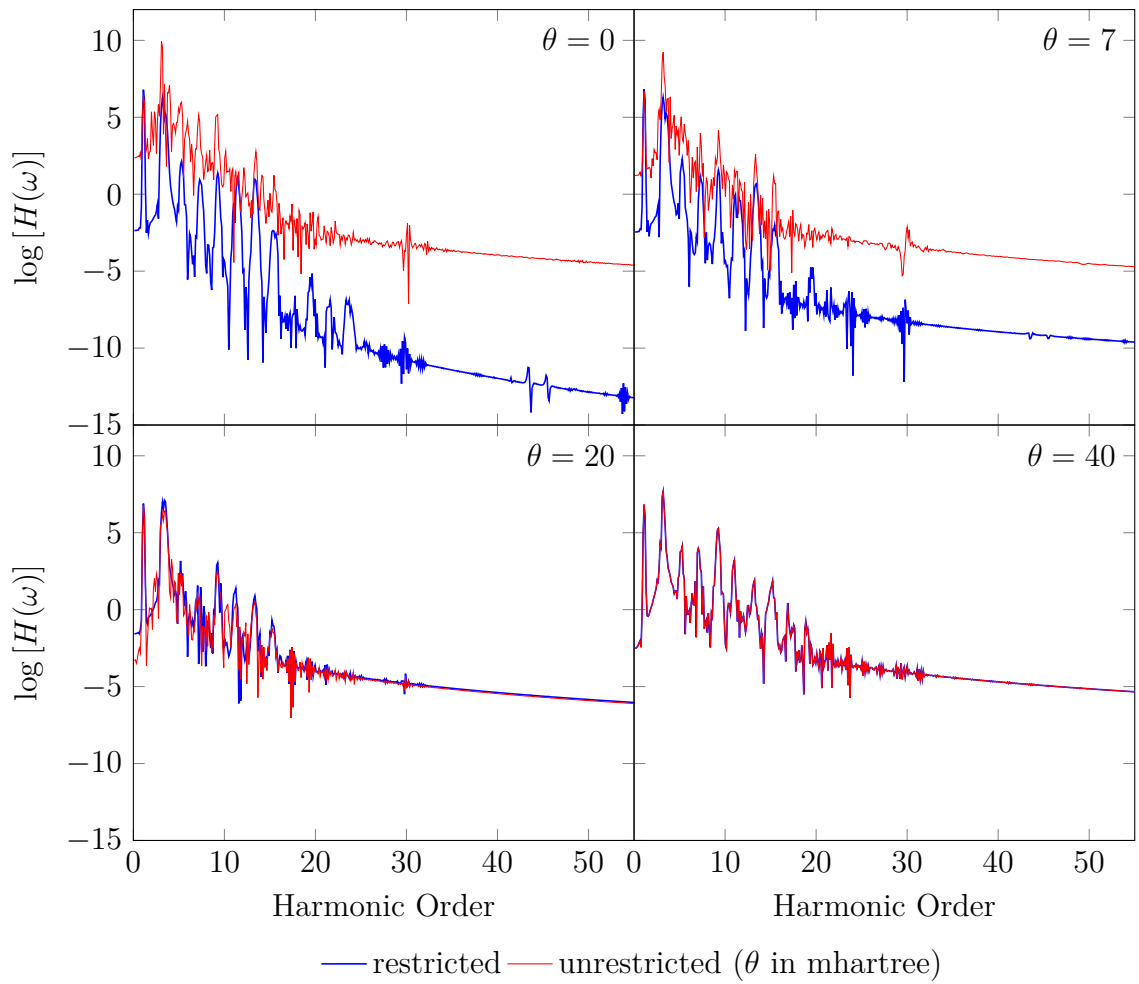


Figure B.8: HHG spectra of H_2 at 3.78 a.u. without window function. $\theta = 0$ corresponds to TDKS-ALDA.

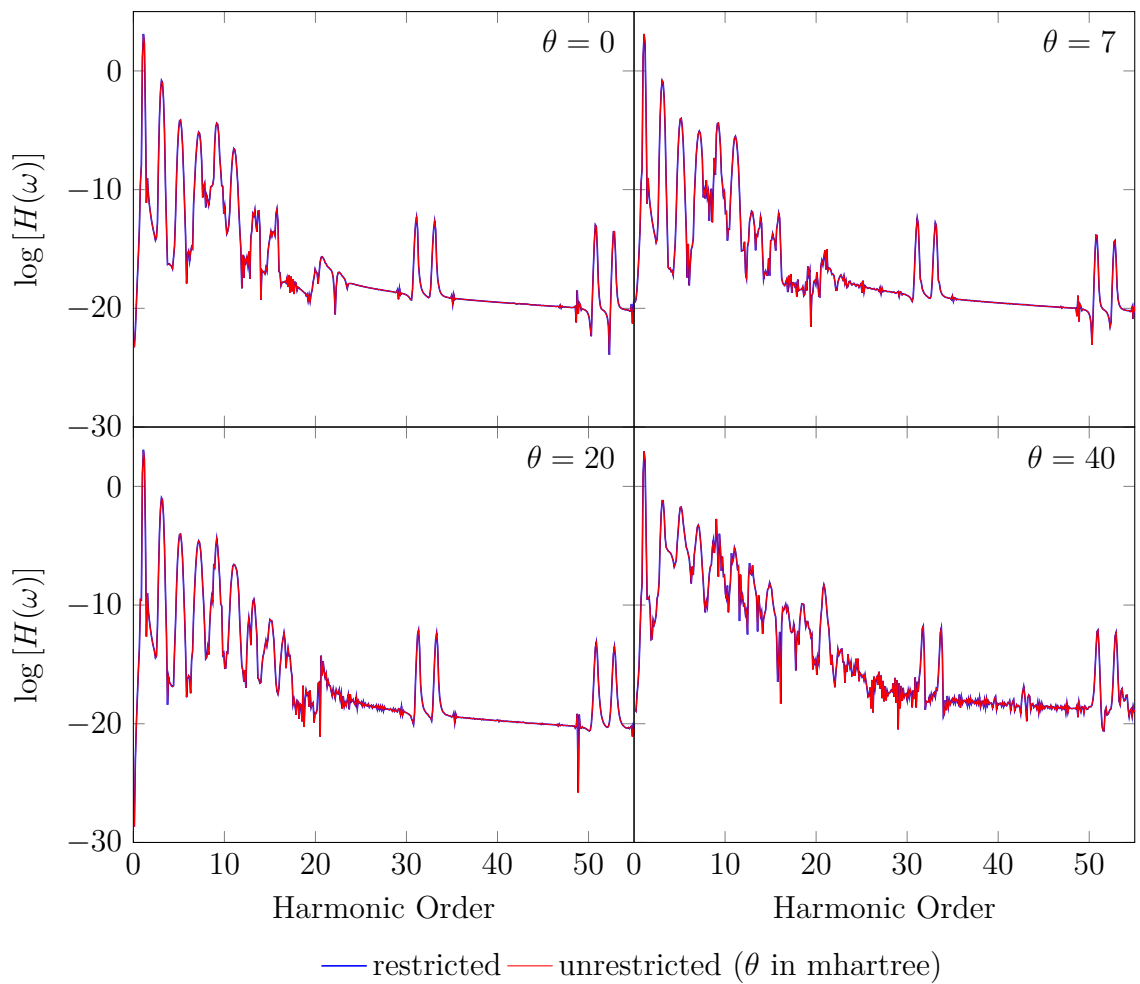


Figure B.9: HHG spectra of H_2 at 1.45 a.u. aligned perpendicular to the laser polarization without window function. $\theta = 0$ corresponds to TDKS-ALDA.

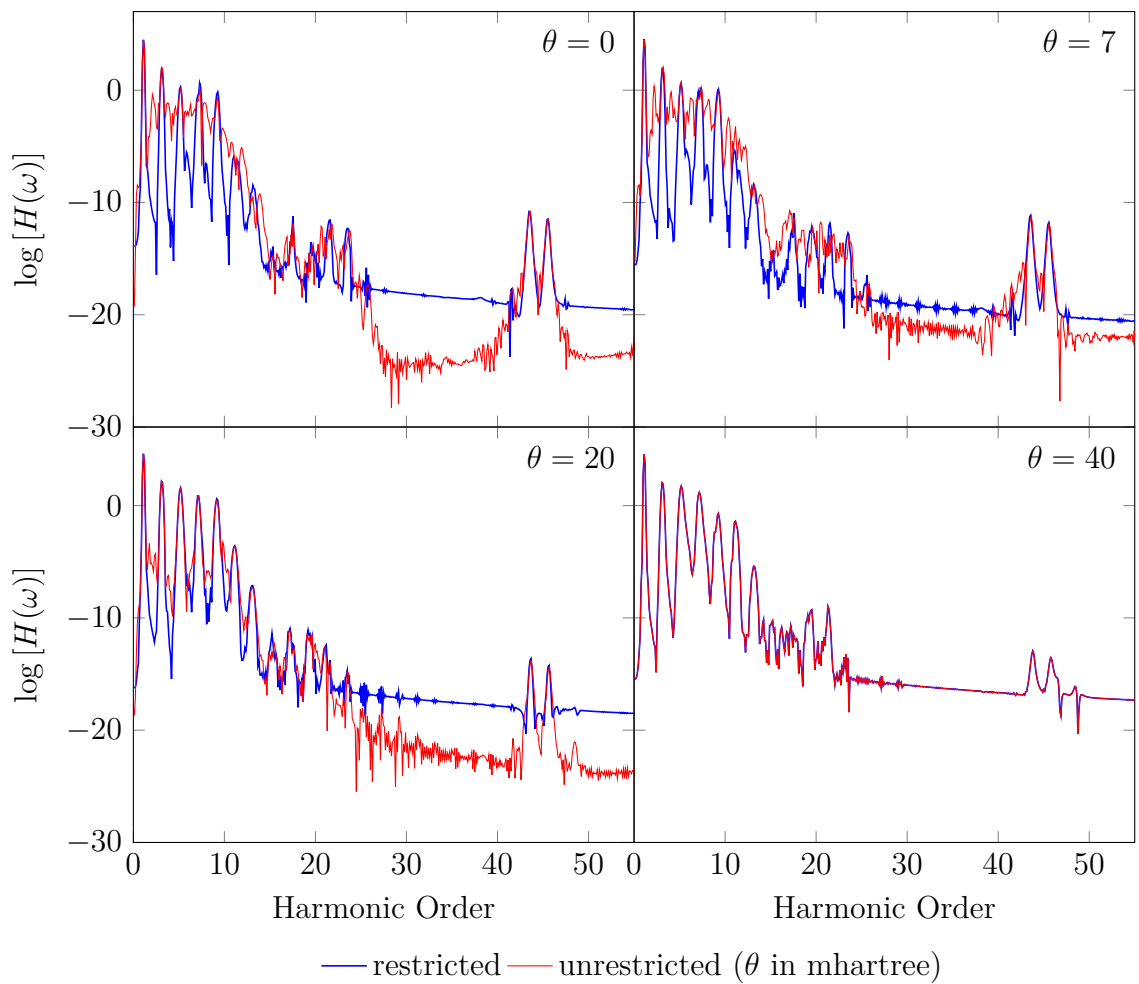


Figure B.10: HHG spectra of H_2 at 3.78 a.u. aligned perpendicular to the laser polarization without window function. $\theta = 0$ corresponds to TDKS-ALDA.